Technical Memorandum ERL NHEML-6

SATELLITE-ESTIMATED RAINFALL IN GATE

William L. Woodley
Cecilia G. Griffith
Joseph S. Griffin
Scott C. Stromatt

National Hurricane and Experimental Meteorology Laboratory
Boulder, Colorado
September 1979

noaa NATIONAL OCEANIC AND ATMOSPHERIC ADMINISTRATION / Environmental Research Laboratories

NOAA Technical Memorandum ERL NHEML-6

SATELLITE-ESTIMATED RAINFALL IN GATE

William L. Woodley
Cecilia G. Griffith
Joseph S. Griffin
Scott C. Stromatt

National Hurricane and Experimental Meteorology Laboratory
Boulder, Colorado
September 1979

UNITED STATES
DEPARTMENT OF COMMERCE
Juanita M. Kreps, Secretary

NATIONAL OCEANIC AND
ATMOSPHERIC ADMINISTRATION
Richard A. Frank, Administrator

Environmental Research
Laboratories
Wilmot N. Hess, Director

CONTENTS

ILLUSTRATIONS

ILLUSTRATIONS (Continued)

TABLES

SATELLITE-ESTIMATED RAINFALL IN GATE

William L. Woodley, Cecilia G. Griffith, Joseph S. Griffin,
and Scott C. Stromatt

Quantitative precipitation estimates have been made for the GARP (Global Atmospheric Research Program) Atlantic Tropical Experiment (GATE) from geosynchronous, infrared satellite imagery and a computer-automated technique that is described in this memorandum. Isohyetal maps and volumetric estimates were made for the GATE A scale (1.43×10^7 km^2) and for a 3° square (1.10×10^5 km^2) that enclosed the B scale for time frames ranging all of GATE (27 June through 20 September 1974) down to 6-hr segments. The estimates for the square are compared with independent rain measurements made by four C-band digital radars that were complemented by shipboard rain gages. The A-scale estimates are compared to rainfall estimates generated by NASA using Nimbus 5 m microwave imagery. Other analyses presented include: (1) comparisons of the satellite rain estimates over Africa with rain gage measurements, (2) maps of satellite-inferred locations and frequencies of new cloud formation, cloud mergers, and cloud dissipations, (3) latitudinal precipitation cross sections along several longitudes, and (4) diurnal rainfall patterns.

The satellite-generated B-scale rainfall patterning is similar to, and the rain volumes are within 10% of, those provided by radar for phases 1 and 3. The isohyetal patterns are similar in phase 2, but the satellite estimates are low, relative to the radar, by 73%. The reasons for this B-scale disparity in phase 2 are unknown, but the analyses presented suggest that it does not carry over to the A scale. Comparison of NASA Electronically Scanning Microwave Radiometer (ESMR) rain estimates with ours for several areas within the A scale for all GATE suggests that the former is low relative to the latter by 50%. The satellite estimates of rainfall in Africa are similar to measurements by rain gages in all phases of GATE up to 11° N and progressively greater than the gage measurements north of this latitude toward the Sahara desert.

The diurnal rainfall studies suggest a midday (about 1200 GMT) maximum of rainfall over the water areas and a late evening maximum (about 0000 GMT) over Africa and the north part of South America. The latitudinal rainfall cross sections along several longitudes by phase clearly show the west-southwest/ east-northeast orientation of the Intertropical Convergence Zone (ITCZ), the diminution of the rainfall west-southwestward from Africa into the Atlantic, and the northward progression of the ITCZ from phase 1 into phases 2 and 3. The center of action for cloud formation, merger and dissipation, and the area of maximum rainfall (exceeding 1600 mm for all of GATE) occurs along the southwest African coast near 11° N. This agrees with past climatologies for this region. Superposition of the satellite-generated rainfall maps and sea surface temperature maps by phase suggests a strong relationship between the two. Almost all of the rainfall occurs within the 26° C sea surface temperature envelope. The mean daily coverage of rainfall and the mean rainfall in the areas with rain for the A scale for all GATE are 20% and 14.1 mm d^{-1}, respectively. These and other results are discussed.

1. INTRODUCTION

Quantitative precipitation estimates have been made for the GARP Atlantic Tropical Experiment (GATE) from geosynchronous, infrared satellite imagery and a computer-automated technique described here. Documentation of the spatial and temporal distribution of the rainfall in GATE was viewed as a prerequisite for the fulfillment of the central objectives of GATE as expressed by Kuettner et al. (1974) before program commencement. As a consequence, several precipitation analysis programs that use various combinations of shipboard radar and rain gages, salinity measurements, atmospheric soundings, and satellite imagery were supported to ensure achievement of the central GATE objectives. Our role was the development and use of a technique to estimate rainfall from satellite imagery in GATE. This study was to culminate in a precipitation atlas (Griffith et al., 1979). The emphasis was on the A scale, because no other method was available for rain estimation on such a large scale (1.43×10^7 km^2). (A variant of the technique has been used by Stout et al., 1979, to make estimates over finer time and space scales.) A-scale satellite rain estimates over smaller areas were compared with those provided independently by other investigators to establish the accuracy and credibility of the satellite-derived rain estimates. The results of the research effort are summarized in this paper and selected products of interest from the atlas are discussed.

2. SATELLITE RAIN ESTIMATION TECHNIQUE

2.1 Satellite Rain Estimation Technique as Developed in Florida

The diagnostic method to estimate rainfall over varying space and time scales in GATE was derived and tested in Florida (Griffith et al., 1978). Based on the finding that time histories of areas of active convection and rainfall in the tropics are brighter or colder on the satellite visible or infrared photographs than those of inactive regions, Applications Technology Satellite (ATS-3) and Synchronous Meteorological Satellite/Geostationary Operational Environmental Satellite (SMS/GOES) images were calibrated with gage-adjusted 10-cm radar data over South Florida. The resulting empirical relationships require a time sequence of cloud area, measured from the satellite images at a specified threshold brightness or temperature, to calculate rain volume over a given period. Only the infrared version of the technique as developed in Florida was used for rain estimation in GATE.

Automation of the technique to computer processing made the production of a GATE rainfall atlas an attainable goal. Automation was accomplished by a series of routines that (1) navigate the satellite after the model of Smith and Phillips (1972) and decrease the spatial resolution, if necessary, (2) isolate and track raining convective clouds with time after the scheme of Wiggert et al. (1976), and (3) calculate and map rainfall over the user-specified region and time period. Use of the tracking software produces time histories of all clouds having top temperatures less than the temperature threshold of 253° K. This software calculates the temporal and spatial locations of cloud origins, mergers, and deaths, as well as cloud size and rain production.

2.2 Satellite Rain Estimation Technique as Applied to GATE

2.2.1 Data

Rainfall in GATE was estimated with the basic technique as developed and tested in Florida. No fine tuning for the GATE environment was done. The data used in this study were the compacted, digital SMS-1 images for GATE provided by Smith and Vonder Haar (1976). The compacted data set covers the area bound by 5° W, 50° W, 5° S, and 22° N (fig. 1); that is, the oceanic portion of the GATE A scale. Both visible and infrared imagery are included in the set at hourly intervals during the 85 days[1] spanning GATE (27 June through 20 September 1974). The infrared data have a spatial resolution of about 4 nmi (about 8 km) north-south and about 2 nmi (about 4 km) east-west and a dynamic range 330° K to 163° K covered by 256 digital counts. This results in a temperature resolution of .5° K below 242° K and 1° K above. The visible data were not used in this study, but have a spatial resolution of about 2 x 2 nmi and a dynamic range of .5 to 100% albedo covered by 64 digital counts.

We processed these 85 tapes of infrared data on the NOAA CDC 6600 computer. Word length on this machine is 60 bits; the machine functions, which allow bit manipulation, were used extensively to pack several variables into one machine word.

Processing 85 days of hourly, full resolution infrared data would have been so costly and time consuming that the task would have been beyond our resources. Yet, analyzing the data at a reduced temporal or spatial resolution would likewise degrade the resolution of the final product rainfall. We balanced these conflicting demands by reducing the spatial resolution to 1/3° latitude by 1/3° longitude (20 nmi x about 20 nmi) grid squares, while saving information about the temperature structure internal to each 1/3° square.

With this technique, clouds are defined as composed of those picture elements that are as cold or colder than 253° K. As described in Griffith et al. (1978), rain volume is a function of temperature, with the colder temperatures implying more rain. Although the relationship between temperature and inferred rainfall is specified continuously for each digital count (that is, for every 1° K), we used only two temperature levels colder than 253° K in computing GATE rainfall. These were 223° K and 213° K. Thus for every 1/3° grid square there were four pieces of information: the average temperature of the square and three values that indicated the fraction of this grid square with temperatures from 253° K through 224° K, 223° K through 214° K and 213° K or colder. Details on the use of this information in rain computations are given in sections 2.2.3 and 2.2.4.

---

[1]No satellite data were available for 22 August 1974.

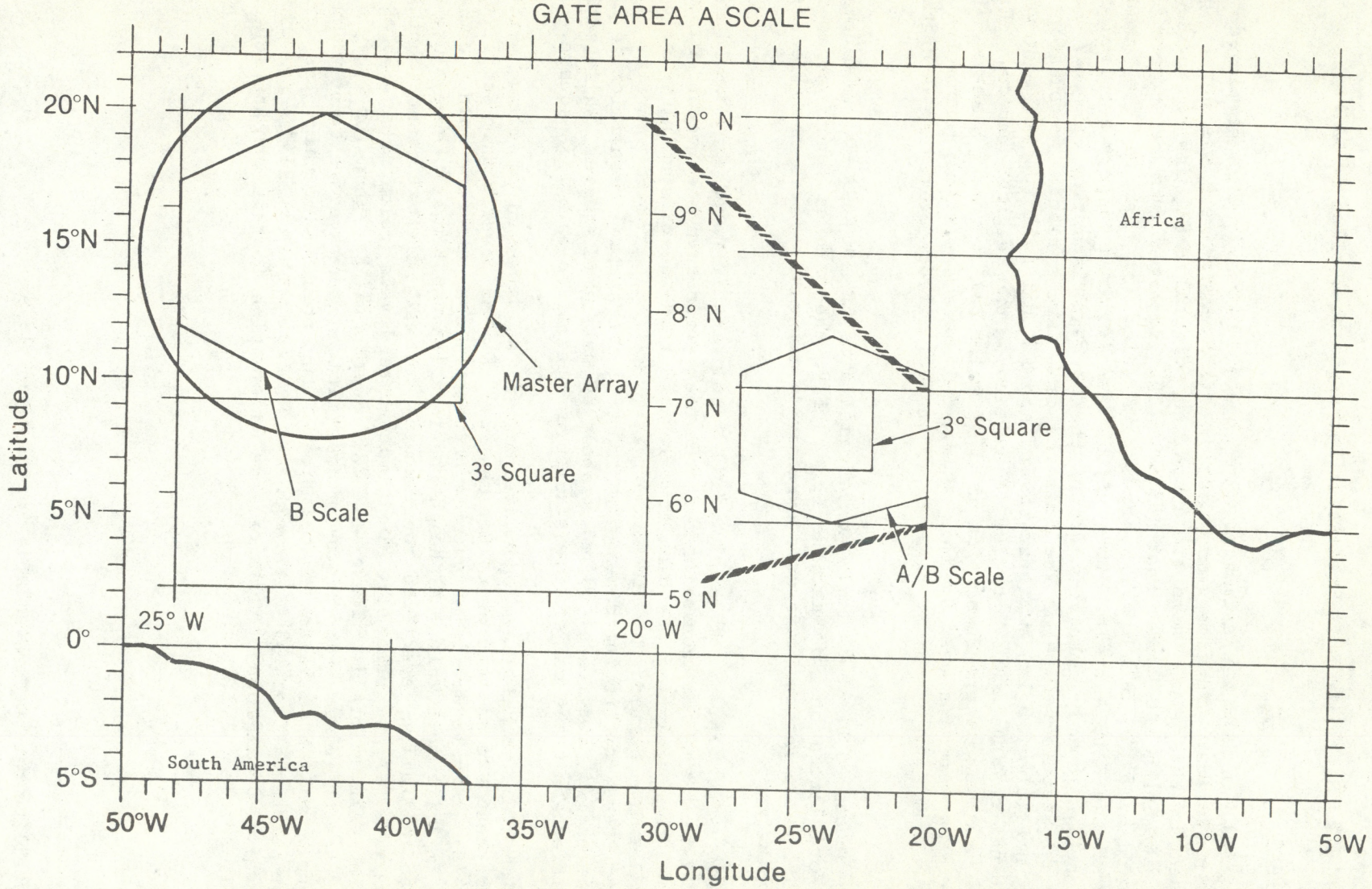

Figure 1. Boundaries of the master array, B-scale hexagon, the 3° square, and the inner polygon. In the enlargement, the circle is the boundary of Hudlow's master array.

2.2.2 SQUISH

Program SQUISH has four functions: (1) calibration of the infrared data, (2) spatial degradation, (3) navigation, and (4) rectilinear remapping. The first function is required because of sensor instabilities in the SMS-1 radiometer and the nonexistence of standard calibration procedures at the time of the GATE. These difficulties are discussed by Smith and Vonder Haar (1976). The calibration routine was kindly provided by Smith.[2]

In the spatial degradation routine, the average temperature in, and fractional coverage of, the three temperature ranges over a "box" are calculated. Up to this point, satellite data are still in the satellite coordinate system and are identified by line (counted from the top of the image) and element (counted from the left side of the image). A box is then composed of 5 lines by 10 elements. The navigation routine (Smith and Phillips, 1972) converts the data from the satellite to an earth coordinate system by determining the latitude and longitude of the center of each box. The sides of the boxes are also determined by a process illustrated in figure 2. The center of a box of interest is shown, as well as the centers of the four nearest boxes. The sides of the box are defined by those lines that are both medians between the box center and the surrounding centers and are parallel to lines of latitude or longitude.

These boxes are mapped onto a 1/3° latitude by 1/3° longitude grid. Rather than simply equivalencing the boxes to the closest 1/3° square, (which would have resulted in holes in the array), we apportioned the average temperature and fractional coverages into each 1/3° square on the basis of fractional overlap of square and box as depicted in figure 2. The disadvantage of this remapping scheme is that there is a small amount (about 2%) of overlap in the 1/3° grid squares at the northwest corner of the A scale.

2.2.3 TRACK

The cloud isolation and tracking routine is that discussed by Wiggert et al. (1976) with parameter values appropriate to the satellite data. Briefly, clouds are defined by the 253°K isotherm and are isolated by an eight-point search method. Once all the grid squares that make up a cloud have been stored, bivariate normal distributions are fitted to the envelope of the cloud and to the areas associated with the temperature relative minima within each cloud (fig. 3). These distributions form the basis for matching clouds between successive images. A match is taken when the area-weighted centroid of the cloud envelope in one frame is within a specified radial distance (2.8 grid squares) of the centroid in the previous frame. If no one-to-one matches fit this criterion, more sophisticated matches are attempted with the distributions for the temperature minima. There are seven categories of matches: tracking old echo (that is, one-to-one matches), lost merged, lost split, lost evaporated, result of merger, result of split, and new growth. We have added

---

[2] E. A. Smith 1977: personal communication.

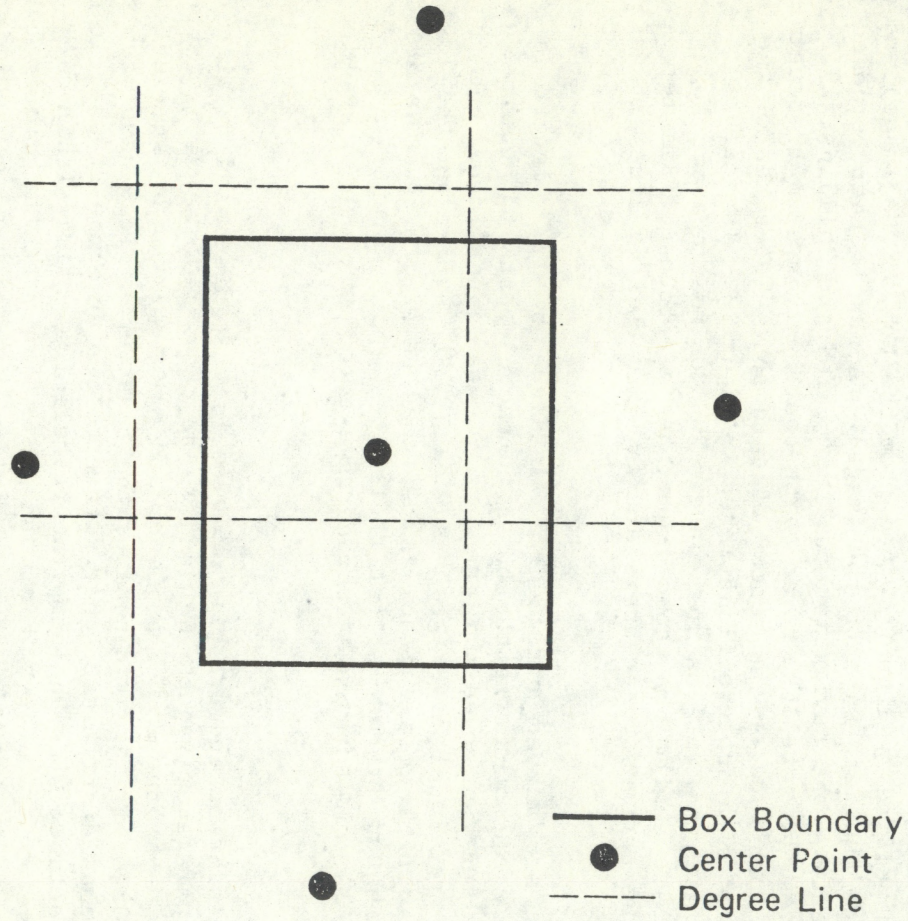

Figure 2. Example of how the boxes were mapped onto the 1/3° latitude by 1/3° longitude grid. For explanation, see text.

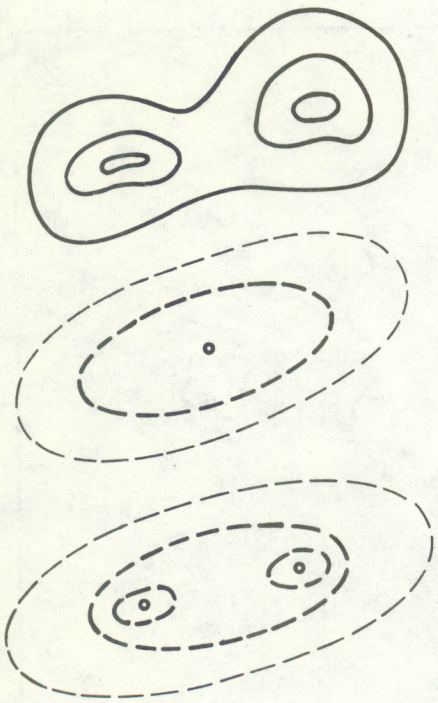

Figure 3. Schematic of a radar echo with two relative maxima (top) and resulting fits from a Fourier algorithm (middle) or a bivariate normal distribution algorithm (bottom). When satellite data are used, contour lines correspond to thermal infrared temperatures or visible brightness levels.

two categories, lost mingle and result of mingle, where a mingle is a cloud that has undergone both merging and splitting from one frame to the next (see fig. 4, frame t_3 to t_4).

2.2.4 TRACER

The output provided by the tracking routine consists of all clouds isolated in each image, as well as cloud size, area weighted centroid, and status indicator (tracking old echo, lost merged, etc.). To make rain calculations, these data must be arranged by individual clouds rather than by image times. Program TRACER accomplishes this rearrangement and prepares the data for rain calculations in program RAINMAP.

To derive this rain estimation technique, a simple model has been assumed in which clouds monotonically grow to a maximum size and then monotonically shrink until they disappear. In the actual rain calculations each image is referenced to maximum cloud area. In practice, few of these simple, single clouds are encountered--most clouds undergo multiple splits, mergers and/or

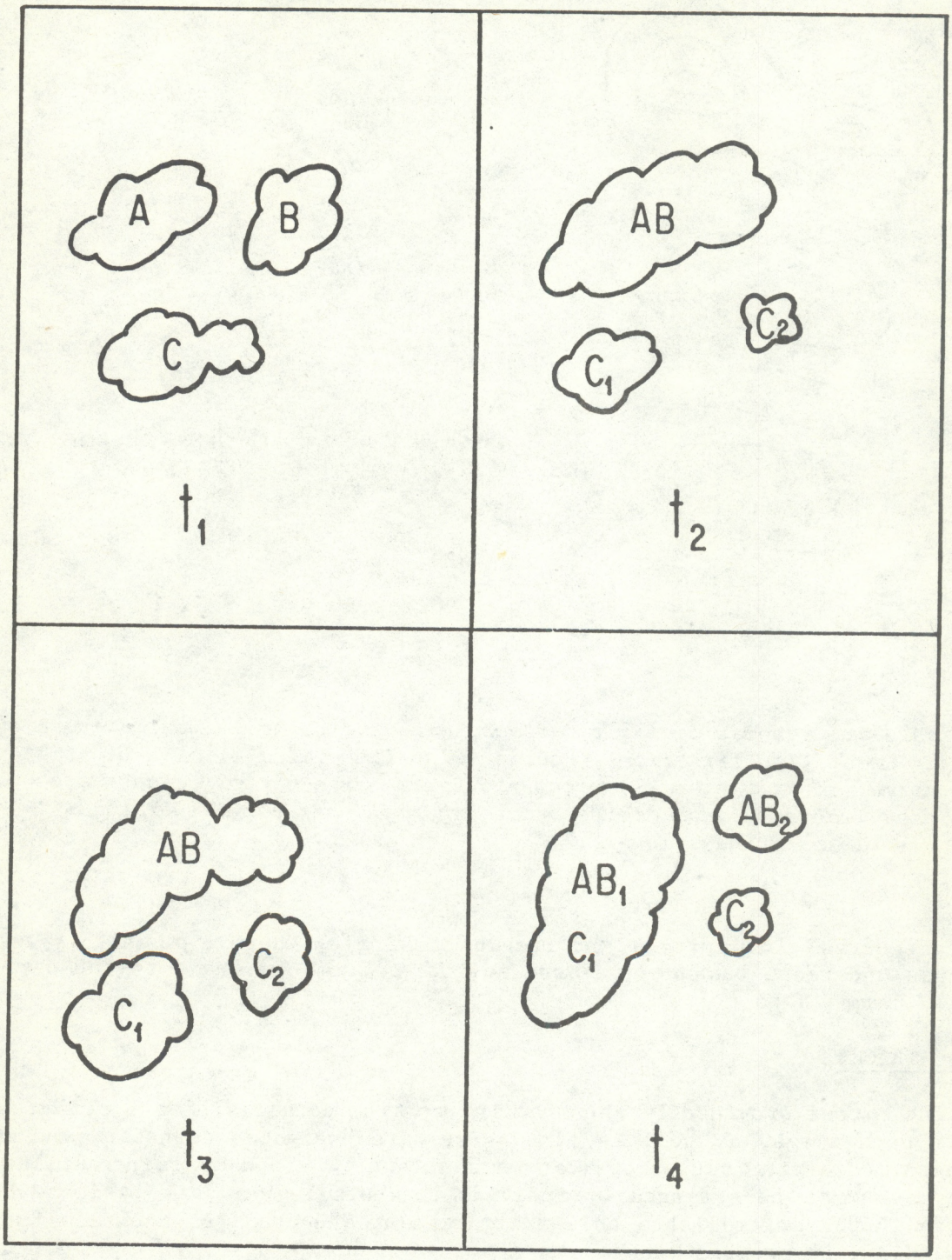

Figure 4. The distinction between "entity" and "segment" cloud histories. For explanation, see text.

mingles[3] during their lifetimes. These types of changes are partly caused by sensor resolution (both spatial and temporal) and cirrus contamination (since the satellite views cloud top), as well as the actual interactions among clouds. In any event, suitable definitions of clouds must be made for these complex interactions. In other uses of this technique (where image sequence spanned, at most, 36 hr) cloud "entities" have been defined as composed of all clouds that at one time had split, merged, or mingled with one another. It is entity area (the sum of the component areas) from which rainfall is computed. In view of the length of the GATE sequence (85 days), the large area of estimation (the A scale), and the degraded spatial resolution used (1/3° latitude by 1/3° longitude), we felt that our previous definition of cloud system was absurd for these time and space scales. As a consequence, for the GATE estimates we have defined cloud "segments." A segment exists as long as cloud status remains "tracking old echo" and terminates when any of the four "lost" codes are encountered.

The distinction between these two definitions can be seen in figure 4 and table 1. In image t_1 there are three clouds. At t_2 the lower cloud has split and the upper clouds have merged. The clouds grow individually in image t_3. In the last frame, the center right cloud has decreased, while the leftmost clouds have mingled; that is, the top left cloud has split into two pieces, one of which has merged with the bottom left cloud. In terms of the entity definition, these clouds form one entity, whereas under the definition of segments there are eight segments in this sequence, as indicated in table 1.

Once all segments have been defined, a rain intensity (H) and total volumetric output (R_v) for each segment at every image time can be computed. The former is computed from

$$H(t_j) = I(t_j) \times A_E(t_j) \times \Delta t \quad , \tag{1}$$

and the latter by

$$R_v(t_j) = H(t_j) \times \sum_{i=1}^{3} \left[a_i(t_j) \times b_i \right] \quad , \tag{2}$$

where t_j indicates the image date and time, I is rain rate (discussed below), A_E is inferred echo area (and is a function of cloud segment size), Δt is the time interval between successive images, a is the fraction of the cloud segment covered by a specified temperature range, b is an empirical weighting coefficient (also a function of temperature), and i_3 indexes the specified temperature range. Both H and R_v have units of m^3. Note that (2) in this paper is formally identical to equation (2) in Griffith et al. (1978). The function I in the latter paper was assigned three values that were functions of echo growth trend (increasing echo size, decreasing echo size, and their average). Using Miami WSR-57 data, we have since refined this

---

[3] A mingle is the simultaneous split and merger of a cloud.

Table 1. Examples of Output From Rain Estimation Programs for the Simulated Case in Figure 5

Cloud tracking output		
Time	ID	Status (frame t_i to t_{i+1})
t_1	A	Lost, merged
	B	Lost, merged
	AB	Result of merger
	C	Lost, split
	C_1	Result of split
	C_2	Result of split
t_2	AB	Tracking old echo
	C_1	Tracking old echo
	C_2	Tracking old echo
t_3	AB	Lost, mingled
	C_1	Lost, mingled
	AB_1C_1	Result of mingle
	AB_2	Result of mingle
	C_2	Tracking old echo

Entity analysis			Segment analysis		
Entity	Time	ID	Segment	Time	ID
1	t_1	A	1	t_1	A
		B	2	t_1	B
		C	3	t_1	C
	t_2	AB	4	t_2	AB
		C_1		t_3	AB
		C_2	5	t_2	C_1
				t_3	C_1

Table 1. Example of Output From Rain Estimation Programs for the Simulated Case in Figure 5 (Continued)

Entity analysis			Segment analysis		
Entity	Time	ID	Segment	Time	ID
	t_3	AB	6	t_2	C_2
		C_1		t_3	C_2
		C_2		t_4	C_2
	t_4	AB_1C_1	7	t_4	AB_1C_1
		AB_2	8	t_4	AB_2
		C_2			

function to take on nine values. As shown in table 2, if echo area is increasing, I assumes one of four values, depending upon what fraction of its maximum size the echo has achieved, and similarly for decreasing echo size.

The fractions a_i are obtained from the fractional coverage of the 1/3° x 1/3° grid square within the three temperature ranges discussed in section 2.2.1. In this manner, subgrid temperature information is used in the calculation of the total volumetric output of a cloud segment or, as shown in section 2.2.5, in the rainfall mapped onto the 1/3° grid squares.

The empirical weighting coefficients have been given in Griffith et al. (1978). For this application, the temperature thresholds were chosen to be 253° K, 223° K and 213° K and b takes on the values 1.00, 2.19 and 3.24, respectively.

2.2.5 RAINMAP

The final product of the estimates originally made by this technique from photographic transparencies was volumetric output (m^3) per cloud per unit time. Since we have started using digital satellite imagery, we have devised several empirical schemes to compute rain depth in those picture elements that make up the cloud and so produce isohyets. For the GATE estimates, cloud area

Table 2. Rain Rate as a Function of Echo Growth Trend for South Florida

Echo growth trend	$I(m^3\ km^{-2}\ h^{-1})$
Increasing area	
$0.0 \leq A_E/A_{EM} < 0.25$	13.3×10^3
$0.25 \leq A_E/A_{EM} < 0.50$	17.3×10^3
$0.50 \leq A_E/A_{EM} < 0.75$	21.1×10^3
$0.75 \leq A_E/A_{EM} < 1.00$	23.8×10^3
$A_E/A_{EM} = 1.00$	20.7×10^3
Decreasing area	
$1.00 > A_E/A_{EM} \geq 0.75$	21.1×10^3
$0.75 > A_E/A_{EM} \geq 0.50$	16.7×10^3
$0.50 > A_E/A_{EM} \geq 0.25$	11.9×10^3
$0.25 > A_E/A_{EM} \geq 0.00$	8.2×10^3

A_E = echo area

A_{EM} = maximum echo area

(defined by the 253° K threshold) and rain area are assumed to coincide.[4] It is further assumed that the colder the grid square is, the more rain it contains. This relationship is specified by the weighting coefficients and the cloud's coverage by the three temperature ranges. Rain depth per 1/3° grid square is calculated for each image by

$$D_{\phi,\lambda}(t_j) = \frac{H(t_j,n)}{10^3 x A_G} \times \sum_{i=1}^{3} \left[\frac{A_{T_i}(t_j,n)}{A_c(t_j,n)} \right] x\ b_i \qquad (3)$$

where $D_{\phi,\lambda}$ is the depth of rain (mm) in the 1/3° grid square indexed by longitude ϕ and latitude λ; A_G is the area (km^2) of this grid square; n is the cloud segment index; A_{T_i} is the area (km^2) of this grid square that is covered by the ith temperature range; and A_c is the total area (km^2) of the cloud segment at this time. The factor of 10^{-3} converts units to millimeters. H, b, and t_j are as before. Hourly rainfall is accumulated and stored in 6-hr periods on tape and 24-hr period accumulations are stored as a paper atlas (Griffith et al., 1979). Both are available from the World Data Center in Asheville, North Carolina.

3. ESTABLISHING A BASIS FOR COMPARISON

No precipitation measurements in GATE, whether they are made by shipboard rain gages, radar, satellite, or a combination of the three can be viewed as absolute standards because of the problems inherent in each system of measurement in an oceanic environment. Nevertheless, through a variety of comparative analyses, a reasonable approximation to the true rainfall can be obtained. As a part of GATE, quantitative precipitation estimates, for an array centered as 8°30' N and 23°30' W, were made during summer 1974 with four C-band digital radars complemented by shipboard rain gages. The results of this precipitation analysis project within the GATE Convection Subprogram were published by Hudlow (1979). Although this analysis project is not without limitations and uncertainties, there is ample justification for using the results of this effort as a basis for comparison with the satellite rain estimates.

Great care was exercised in the derivation of the radar rainfall analyses. The electronic calibrations of the GATE radars were established before the GATE field operations and were routinely checked throughout the experiment. The radar calibrations were evaluated through analyses that included comparisons of measurements from two or more radars in regions of overlapping coverage and comparisons of radar rainfall estimates with shipboard rain gage measurements (Hudlow et al., 1979; Hudlow and Patterson, 1979).

---

[4] In other applications that use the full resolution data, we have found it physically more reasonable to assume that the rain area is some fraction of the cloud area.

The rainfall amounts that reached the sea surface were estimated by means of the low-altitude radar data sets. A Cartesian data array with the elemental data bin sizes equal to 4 km x 4 km was adopted and the Cartesian arrays of calibrated and validated reflectivity data from the individual radars served as data input to the primary precipitation software system. These data were normally available every 15 min. The output from the primary precipitation software was hourly accumulated rainfall maps for a master array that covered a circle 204 km in radius navigated to an origin at 8°30' N and 23°30' W which was also the center of the GATE B-scale array. For phases 1 and 2 of GATE, only the radar data sets from the *Researcher* and *Oceanographer* were used to derive the hourly precipitation maps. According to Hudlow (1979), this decision was based on data availability, ship location, and the superior range performance of the *Oceanographer* radar. To cover the master array during phase 3, data from all four radars (*Researcher, Oceanographer, Quadra,* and *Gilliss*) were merged when available. The data processing to obtain precipitation is discussed extensively by Patterson et al. (1978) and in lesser detail by Hudlow (1979). Hudlow et al. (1979) describe the techniques for calibrating and comparing the radars and the manner in which the various biases were determined and removed before the data from the individual radars were merged.

Hudlow and Patterson compared, extensively, the radar rain estimates with shipboard rain gages. They concluded that "matching the gage and radar values could best be done by minimizing the difference between the gage value and a radar estimate selected from a small set of radar data bins comprised of the one containing the mean gage position and the closest adjoining data bins." Even so, they recognized the difficulty in assessing absolute errors based upon sparse shipboard rain gages that had miniscule sampling volumes compared with the radar. The results of the comparisons between the merged radar data and the shipboard rain gages are summarized in table 3, which was extracted from Hudlow, 1979 (his table 4). The mean absolute percentage difference between the gage and radar values was calculated from

$$\Sigma\Sigma \left| \frac{(\text{gage}_{ij} - \text{radar}_{ij})}{\text{gage}_{ij}} \right| \times 100/N \quad , \tag{4}$$

where the sums are for all B-scale stations (i) used in the analysis and for all phases (j), or days (j), during GATE; N is the total number of gage-radar pairs. It would appear that removal of systematic biases, which were < 3 dB, before the merger of the data resulted in a data set that compares favorably with the rain gage measurements. The mean absolute percent differences are about 15% for the phase rain estimates and about 25% for the daily and hourly rain estimates.

Although not a perfect standard, there can be little doubt that the radar estimates of rainfall complemented by rain gages for the master array are the best possible under the circumstances. Table 3 suggests that this standard is most reliable for the various phases and less so for individual days or hours

Table 3. Summary of Mean Absolute Percent Differences Between Radar and Shipboard Rain Gage Measurements (from Hudlow, 1979)

Scales		Mean absolute percent difference (error)	Comments
Time	Space		
Phase	16 km^2	14%	Each radar estimate was taken as the value in closest agreement with the rain gage, from the set of four 4 km x 4 km data bins consisting of the one containing the phase mean ship position plus the three nearest neighboring bins.
Daily	16 km^2	23%	Each radar estimate was taken as the value in closest agreement with the rain gage, from the set of nine 4 km x 4 km data bins consisting of the one containing the daily mean ship position plus the eight surrounding bins.
1-3 hr	$5 \times 10^2 - 5 \times 10^3$ km^2	23%	Based on expected range of space scales over which the 4-km radar estimates must be averaged to obtain an accuracy equivalent to the daily estimates for time scales of 1-3 hr.

within the phases when random errors might prove to be dominant. These uncertainties should be kept in mind when the comparisons of the satellite rain estimates with this standard are interpreted later in the paper.

4. SATELLITE-DERIVED RAINFALL ESTIMATES FOR GATE

4.1 Accuracy of B-Scale Estimates

Satellite-derived daily rain estimates for the 3° square (22° to 25° W and 7° to 10° N) that encompasses the GATE B scale and for the GATE A scale (fig. 1) for the 85 days between 27 June and 20 September 1974 are provided in table 4. Radar rain estimates for the 3° square, obtained from the merged data set, are provided when available. The ratios of satellite to radar values (and vice versa) are included as well. For 6-hourly rain estimates within the day, the reader is referred to the GATE rain atlas (Griffith et al., 1979). According to the satellite rain estimates, the wettest day in the 3° square was 20 August (day 232) with 0.54×10^{10} m^3 of rain. (Day 232 was an interphase day between phases 2 and 3.) Over the A scale, 19 September (day 262) was the wettest with 9.46×10^{10} m^3.

Plots of daily and cumulative satellite and radar-derived rainfalls by phase for the 3° square are provided in figures 5, 6, and 7. Note that the ratio of satellite to radar rainfalls is provided in the cumulative plots. The break in the plots for phase 2 (fig. 6) is caused by a lack of radar data when the *Oceanographer* was off station because of a medical emergency. The agreement between satellite and radar is remarkably good in phases 1 and 3, but rather poor in phase 2 when the satellite rain estimates are systematically low relative to the radar estimates, amounting to 73% by the end of the phase. The third (dotted) curve in the daily plots for phase 2 (fig. 6a) shows the daily values one would obtain by adjusting all the satellite rainfall estimates upward by a factor of 1.73. As we will see, there is little justification for applying this type of adjustment.

Plots of the satellite-inferred, daily rain volumes for the GATE A scale for the three phases are provided in figure 8. The "adjusted" curve for phase 2 was obtained by increasing all of the A-scale estimates by 73% based upon the radar-satellite comparisons for the 3° square in the same period. An examination of the plots suggests that this adjustment is not appropriate for the A scale because the adjusted curve appears to be anomalous when compared to the unadjusted curves for the other phases.

These general impressions are reinforced by a study of tables 5 and 6. Table 5 summarizes phase rain estimates from the gage, radar, and satellite data sets. The satellite and radar rainfalls were summed over the 3° square, and the area average computed. The rain gage data were taken from Hudlow (1977), where mean hourly rainfall rates (mm h^{-1}) are shown by phase for each ship. An area-average rainfall rate was computed and the value was multiplied by the appropriate number of hours in the phase to produce the B-scale average depths provided in table 5.

Table 4. Satellite-Derived Daily Rain Estimates for GATE 3° Square and A Scale (27 June - 20 September 1974)

	Day	Hour	3° Square Rainfall ($m^3 \times 10^8$) Radar	Satellite	Ratio R/S	S/R	A-Scale Satellite ($m^3 \times 10^{10}$)
Phase I	178	00-24		3.08			7.66
	179	00-24	22.81	37.86	0.60	1.66	8.91
	180	00-24	15.28	24.99	0.61	1.64	6.36
	181	00-24	10.71	1.72	6.23	0.16	4.38
	182	00-24		9.62	0.72	1.39[1]	3.26
	183	00-24	33.69	32.71	1.03	0.97	4.41
	184	00-24	6.35	2.42	2.62	0.38	3.88
	185	00-24	3.60	1.87	1.92	0.52	2.58
	186	00-24	0.60	0.03	20.00	0.05	2.87
	187	00-24	1.66	0.02	83.00	0.01	3.27
	188	00-24	44.40	26.93	1.65	0.61	3.29
	189	00-24	18.92	18.37	1.03	0.97	3.56
	190	00-24	1.06	0.28	3.79	0.26	3.43
	191	00-24	0.061	0.20	0.30	3.28	3.20
	192	00-24	0.37	0.002	185.00	0.005	3.30
	19.	00-24	1.11	5.04	0.22	4.54	6.04
	194	00-24	20.72	11.61	1.78	0.56	5.43
	195	00-24	20.28	15.59	1.30	0.77	6.18
	196	00-24	9.49	11.72	0.81	1.23	4.60
	197	00-24	1.28	0		0	1.77
Interphase Days	198	00-24		0			4.25
	199			14.24			7.71
	200	00-24		45.92			6.71
	201	00-24		10.54			4.48
	202	00-24		0.65			1.99
	203	00-24		29.85			2.76
	204	00-24		7.28			4.53
	205	00-24		1.09			4.23
	206	00-24		4.96			6.55
	207	00-24		6.11			3.97
	208	00-24		13.78			5.32
Phase II	209	00-24	28.31	17.65	1.60	0.62	5.01
	210	00-24	9.57	6.57	1.46	0.69	2.34
	211	00-24	4.81	0.65	7.40	0.14	2.41
	212	00-24		0.78			3.51
	213	00-24		10.67			3.13
	214	00-24		11.68	0.65	1.54[2]	4.48
	215	00-24	7.00	2.33	3.00	0.33	2.88
	216	00-24	4.31	0.74	5.82	0.17	1.98
	217	00-24	12.08	2.70	4.47	0.22	2.15
	218	00-24	3.20	1.35	2.37	0.41	4.05
	219	00-24	4.75	2.60	1.83	0.55	5.28
	220	00-24	12.43	5.73	2.17	0.46	5.45
	221	00-24	5.42	5.97	0.91	1.10	8.36
	222	00-24	19.56	9.74	2.01	0.50	3.04
	223	00-24	0.43	1.44	0.33	3.00	3.88
	224	00-24	28.94	28.30	1.02	0.98	5.06
	225	00-24	12.76	2.54	5.02	0.20	3.83
	226	00-24	0.80	1.47	0.54	1.84	1.95
	227	00-24	0.73	0		0	3.78
Interphase Days	228	00-24		2.10			4.65
	229	00-24		12.18			6.06
	230	00-24		5.69			3.67
	231	00-24		12.84			2.51
	232	00-24		53.97			4.24
	233	00-24		5.55			3.67

[1]Ratio calculated from 18 hrs of data.

[2]Ratio calculated from 6 hrs of data.

Table 4. Satellite-Derived Daily Rain Estimates for GATE 3° Square and A Scale (27 June - 20 September 1974) (Continued)

	Day	Hour	3° Square Rainfall ($m^3 \times 10^8$) Radar	Satellite	Ratio R/S	Ratio S/R	A-Scale Satellite ($m^3 \times 10^{10}$)
	234	NO DATA FOR THIS DAY					
	235	00-24		25.48		4.57	
	236	00-24		20.43			6.94
	237	00-24		11.21			4.33
	238	00-24		3.39			4.56
	239	00-24		1.25			4.18
	240	00-24		17.19			5.90
	241	00-24		32.07			5.52
Phase III							
	242	00-24	15.73	15.54	1.01	0.99	4.57
	243	00-24	2.10	0.43	4.88	0.20	1.58
	244	00-24	0.73	0.01	73.00	0.014	2.70
	245	00-24	26.90	21.80	1.23	0.81	4.60
	246	00-24	2.71	1.94	1.40	0.72	7.97
	247	00-24	18.52	26.05	0.71	1.41	5.76
	248	00-24	25.22	24.36	1.04	0.97	4.20
	249	00-24	7.20	8.14	0.88	1.13	5.81
	250	00-24	4.32	0.09	48.00	0.02	6.94
	251	00-24	7.57	7.94	0.95	1.05	5.81
	252	00-24	14.66	11.93	1.23	0.81	4.41
	253	00-24	2.25	0.78	2.88	0.35	5.18
	254	00-24	3.03	4.14	0.73	1.37	3.39
	255	00-24	15.39	22.80	0.68	1.48	4.65
	256	00-24	16.49	16.37	1.01	0.99	5.31
	257	00-24	21.43	19.12	1.12	0.89	4.79
	258	00-24	5.46	1.57	3.48	0.29	4.28
	259	00-24	22.89	20.33	1.13	0.89	4.94
	260	00-24	13.81	16.90	0.82	1.22	5.96
	261	00-24	2.53	0.82	3.09	0.32	4.80
	262	00-24		30.47			9.46
Interphase Day	263	00-24		23.47			7.21
Phase I	178 to 197	00-24	218.63	200.02 (200.98)	1.09	0.92	88.68
Phase II	209 to 227	00-24	155.15	89.78 (112.91)	1.73	0.58	72.57
Phase III	242 to 262	00-24	228.94	221.06 (251.53)	1.04	.97	110.11
Phases I, II, III		00-24	602.72	511.66	1.18	0.85	271.36
ALL GATE	178 to	00-24		929.65			391.67

(Phase totals for the 3° square are for all days with 12 hr or more of data. The totals in parentheses and the A-scale totals include all days within the phase.)

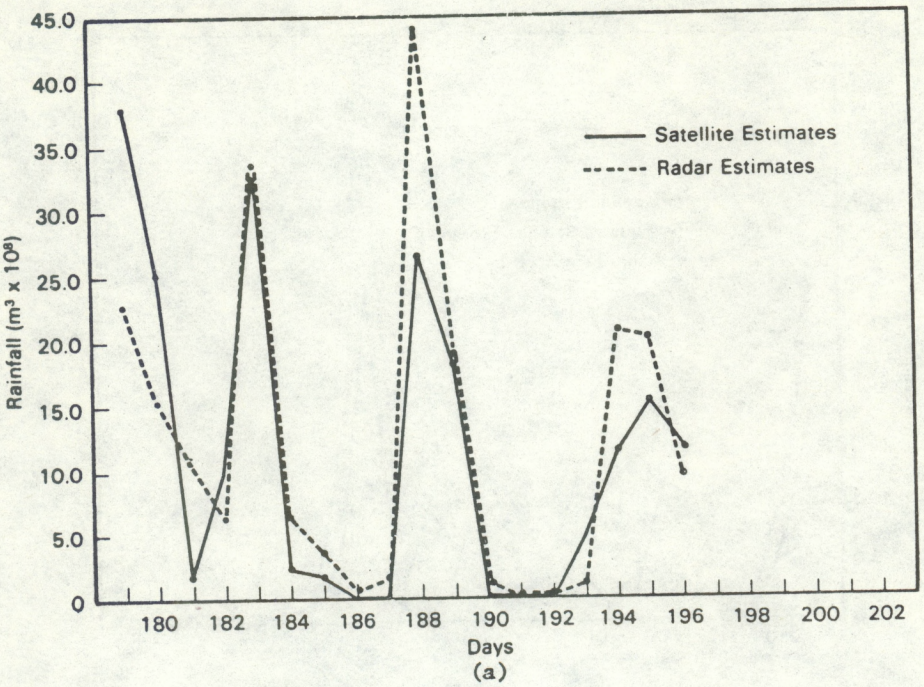

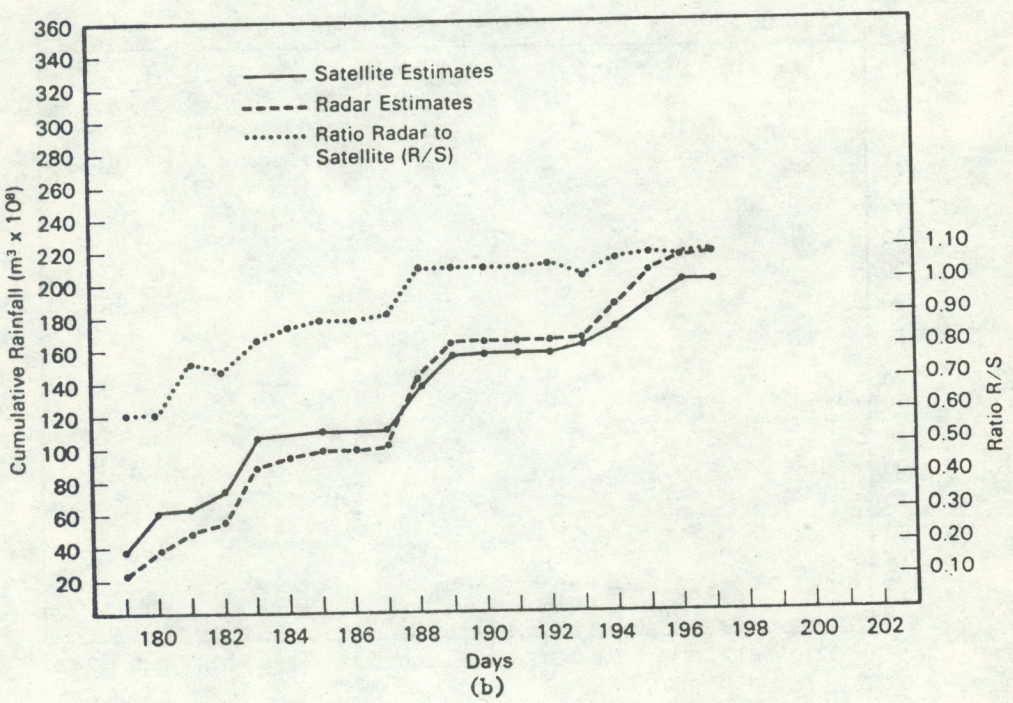

Figure 5. Phase 1 rain volume estimates for the 3° square from satellite and radar: (a) daily, and (b) cumulative.

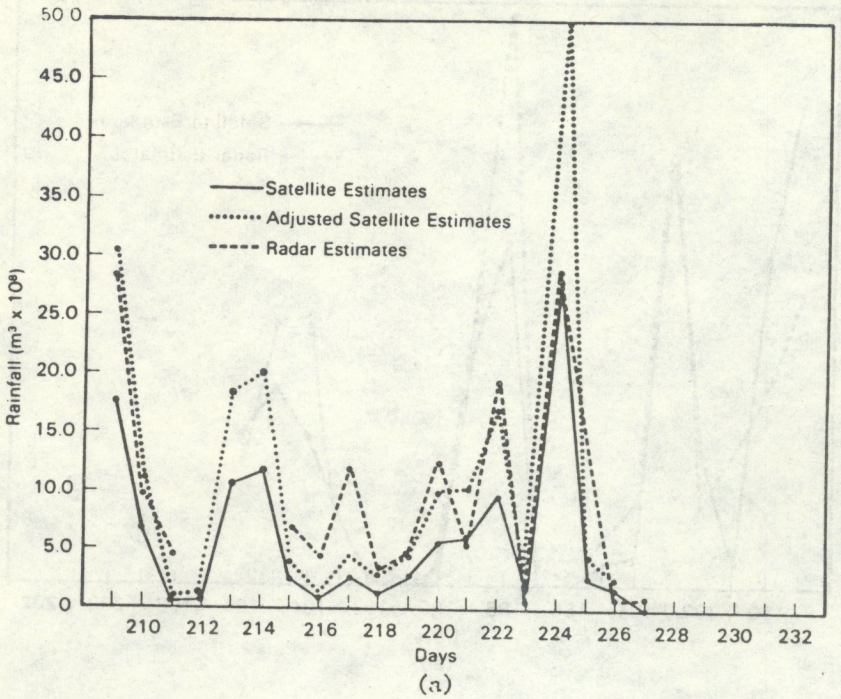

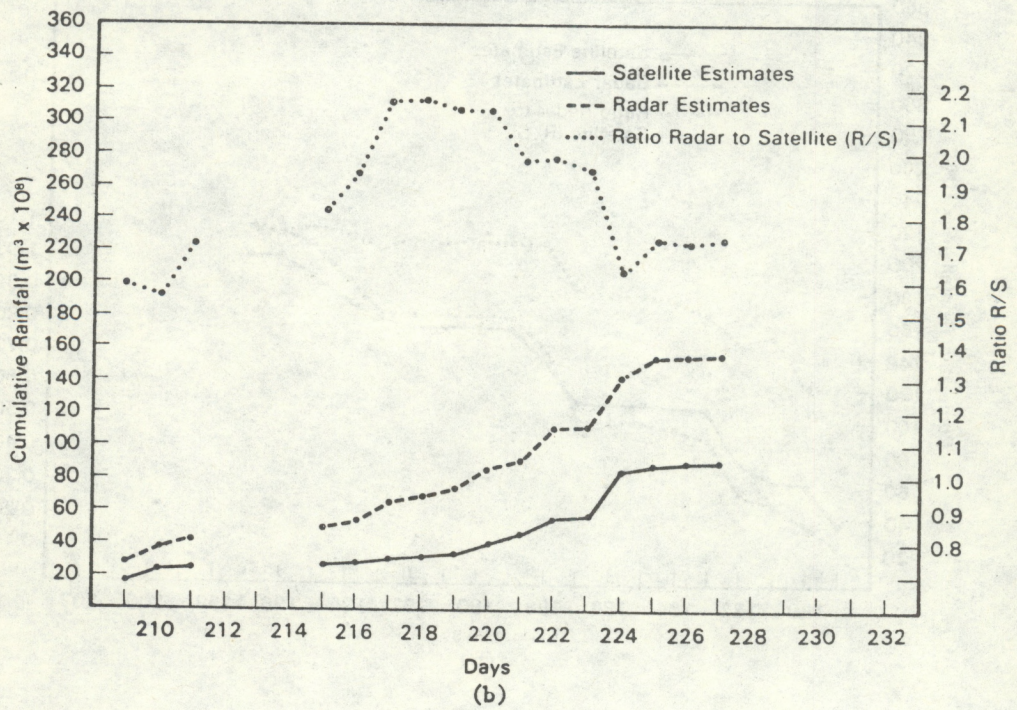

Figure 6. Phase 2 rain volume estimates for the 3° square from satellite and radar: (a) daily, including adjusted satellite estimates, and (b) cumulative.

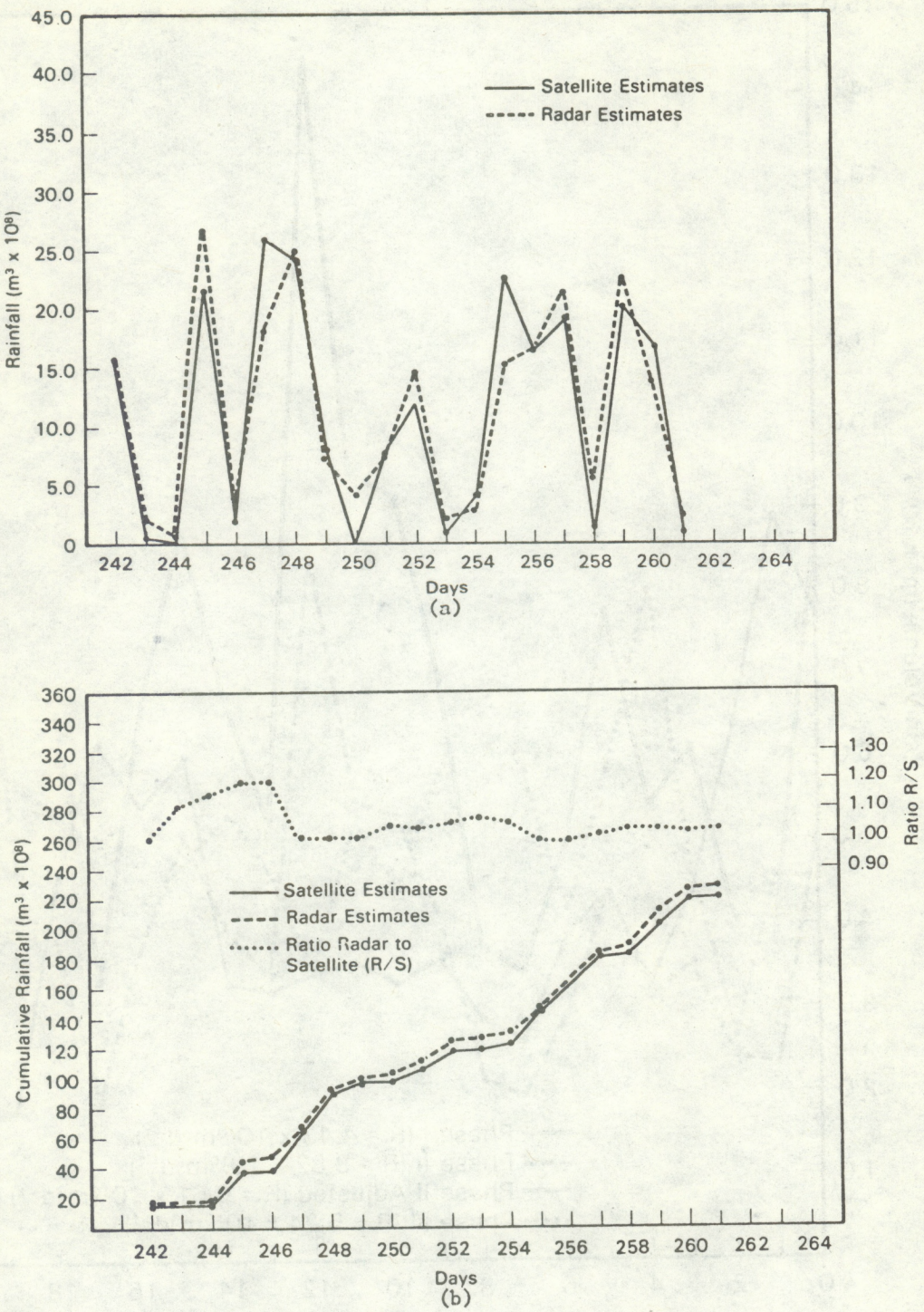

Figure 7. Phase 3 rain volume estimates for the 3° square from satellite and radar: (a) daily, and (b) cumulative.

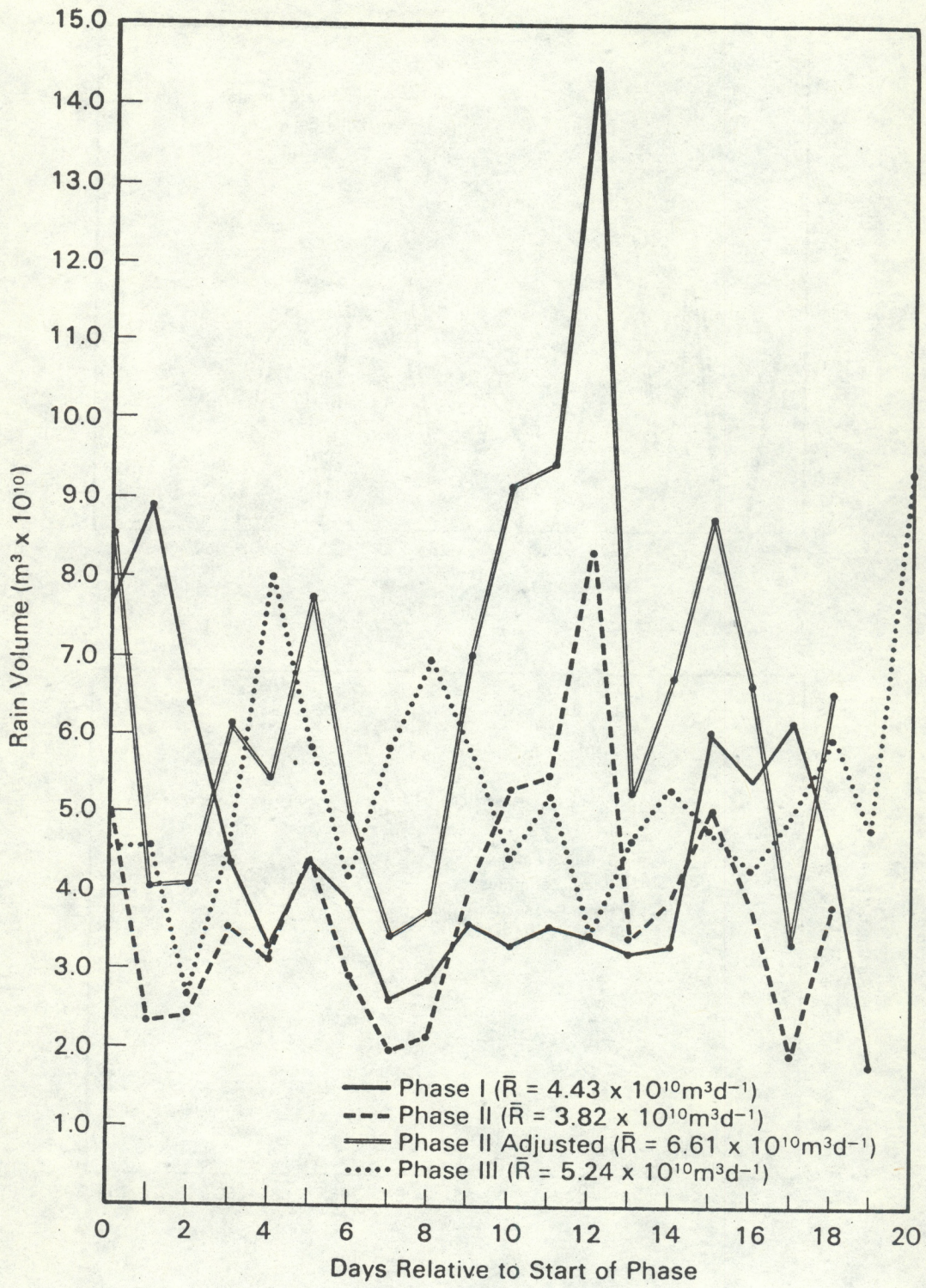

Figure 8. Satellite-estimated daily A-scale rain volumes for phase 1, phase 2, adjusted phase 2, and phase 3.

Table 5. Phase Rainfall Comparisons for the 3° Square

Phase	Gage vs. radar (mm x 10^8)			Gage vs. satellite (mm x 10^8)			Radar vs. satellite (m^3 x 10^8)		
	Gage	Radar	G/R	Gage	Satellite	G/S	Radar	Satellite	R/S
1	204.6	193.7	1.06	204.6	178.0	1.15	218.6	201.0	1.09
2	131.7	137.4	0.96	131.7	79.5	1.66	155.2	89.8	1.73
3	215.6	202.8	1.06	215.6	195.8	1.10	228.9	221.1	1.04

Table 6. Daily Phase Rainfall Parameters

Rainfall parameters	Radar (m^3x10^8) (3° square)			Satellite (m^3x10^8) (3° square)			Satellite (m^3x10^{10}) (A-scale)		
Phases:	1	2	3	1	2	3	1	2	3
Maximum	44.40	28.94	26.90	37.86	28.30	26.05	8.91	8.36	9.46
Minimum	0.06	0.48	0.73	0.00	0.00	0.01	1.77	1.95	1.70
Median	7.92	6.21	10.69	5.04	2.57	10.04	3.57	3.78	2.70
Mean	11.51	8.62	11.45	10.58	4.99	11.05	4.26	3.82	5.24

The radar estimates agree quite well with the gage estimates for the phases, but this was expected since systematic biases for the various radars (determined in many cases by comparison with rain gages) were removed before merger of the data. As noted, the satellite estimates agree quite well with the rain gage and radar estimates for phases 1 and 3, but are low relative to the others in phase 2.

Based upon the results presented so far, it appears that it is the satellite estimates and not the radar estimates for the 3° square that are anomalous in phase 2. Table 6, a summary of simple statistical parameters for the radar and satellite rainfalls, tends to support this conclusion. The rainfall ranges (that is, maxima and minima) are comparable for the satellite and radar, but the phase 2 median and mean values as obtained from the satellite appear anomalously low. However, no such anomaly is evident in the A-scale satellite values presented in table 5, and it is obvious that adjustment of the A-scale values based on the B-scale comparisons would degrade the satellite estimates for the A scale.

Why the satellite rainfall estimates are apparently degraded for just the B scale in phase 2 is not known definitively. If the explanation is meteorological, it is apparently a problem only for the B scale. It is interesting that three independent weather classifications of GATE days by J. Dewart, E. Smith, and D. Loranger[5] of Colorado State University suggest that the weather of phase 2 in the B scale was different from the weather of phases 1 and 3. Using satellite images, radar analyses, gage data, and radiometric measurements, they typified days as convectively suppressed, convectively enhanced, stratiform cloudiness or other. Most of the phase 1 and 3 days fell into the first two categories, whereas most of the phase 2 days fell into the latter two (that is, stratiform or other). If these classifications are accurate, the performance of the satellite rain estimation technique in phase 2 would be explained, since the technique was developed primarily for convective situations and not for stratiform rains.

A performance assessment of the satellite technique relative to the radar for the 3° square in all phases can be made by studying the scatter plot of daily rainfalls and regression in figure 9. The two variables are obviously strongly related, having a correlation coefficient of 0.87. In general, a day identified as wet with the satellite was, in fact, wet as estimated by radar, and conversely for the dry days. This result increases the credibility of the satellite rain estimates for the A scale.

The mapped radar and satellite daily rainfall products in the GATE rain atlas (Griffith et al., 1979) were compared qualitatively and quantitatively. On most days there was good correspondence; that is, the general patterns were recognizable and the relative maxima corresponded in both products. However, the satellite maps usually had more extensive rain coverage, but lower point maxima, when compared to the radar maps. The latter is quantified in

---

[5] J. Dewart, E. Smith, and D. Loranger 1978: personal communications.

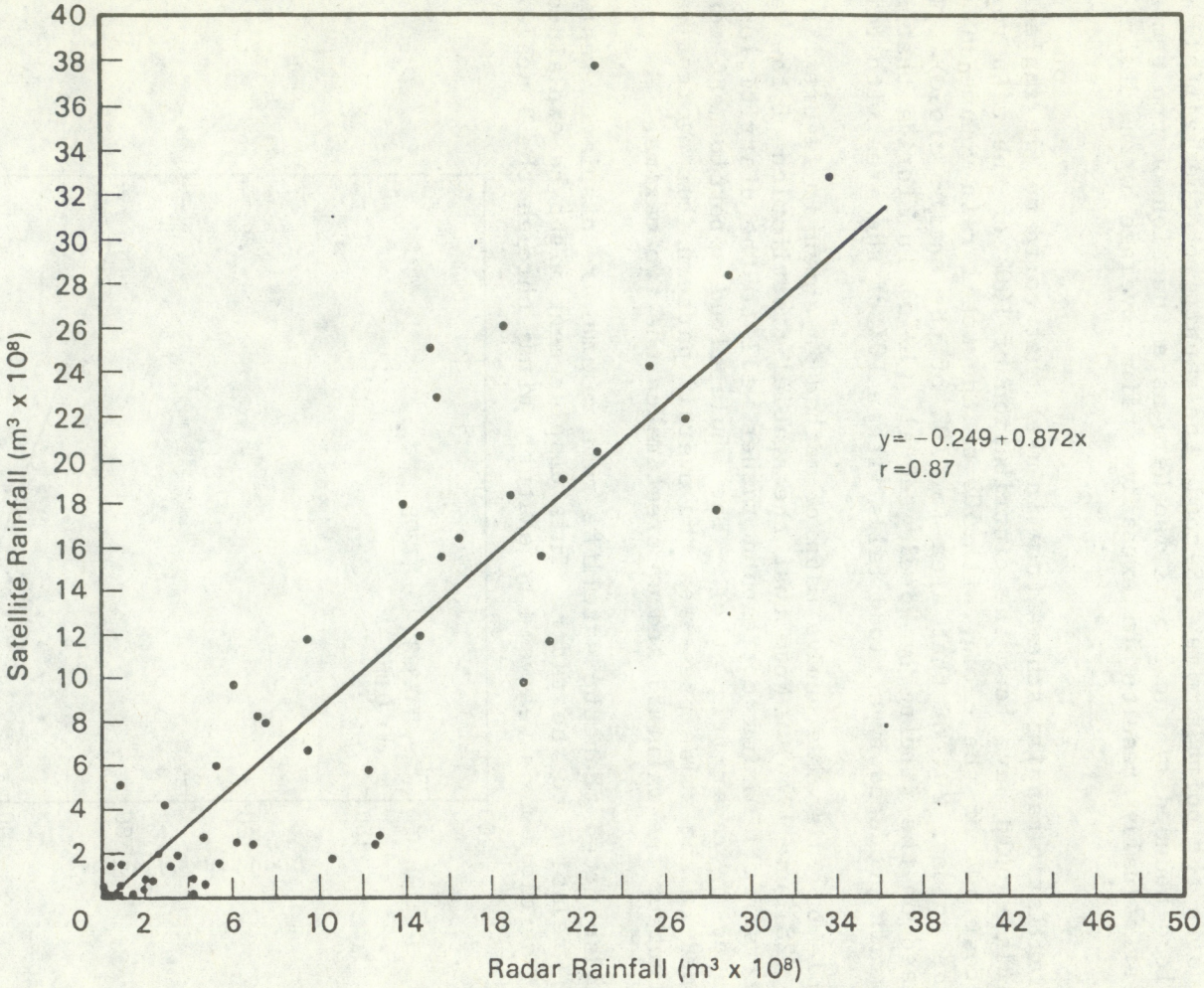

Figure 9. Scatter plot and regression of satellite versus radar daily rain volumes for all phases over the 3° square.

scatter plots and regressions between satellite and radar-measured maxima for the three phases (fig. 10).

Lower satellite point maxima were expected for two reasons. First, the deliberate degradation of the satellite resolution to 1/3° x 1/3° squares was certain to smooth the point maxima. Second, the mapping of the rainfall over the entire cloud bounded by the 253° K isotherm as a function of top temperature characteristically results in excessive rain coverage with diminished point maxima.

A more realistic mapping scheme (now in use) that could not be implemented for the atlas would have been the distribution of 100% of the rain volume over the coldest 50% of the cloud, with 50% of the total rain volume distributed over the coldest 20% of that area (or 10% of the entire cloud). This scheme is based on the finding by Woodley et al. (1975) in Florida that half (50%) of the rain produced by a cloud falls within 10% of the area with rain.

An example of this alternative mapping method is shown in figure 11b for GATE day 179 (28 June 1974). Note that the spatial distribution of the rainfall and the rainfall maxima correspond rather well to the distribution and maxima estimated by radar (fig. 11c). The whole cloud apportionment method (fig. 11a) used in the atlas preserves the overall pattern, but overestimates the areal extent of the rainfall and underestimates the two maxima.

It was also noted that the satellite rain maxima are displaced westward by 1/4° to 1/2° relative to the radar. This displacement might be explained by advection of the cloud tops westward by easterly winds through the B scale.

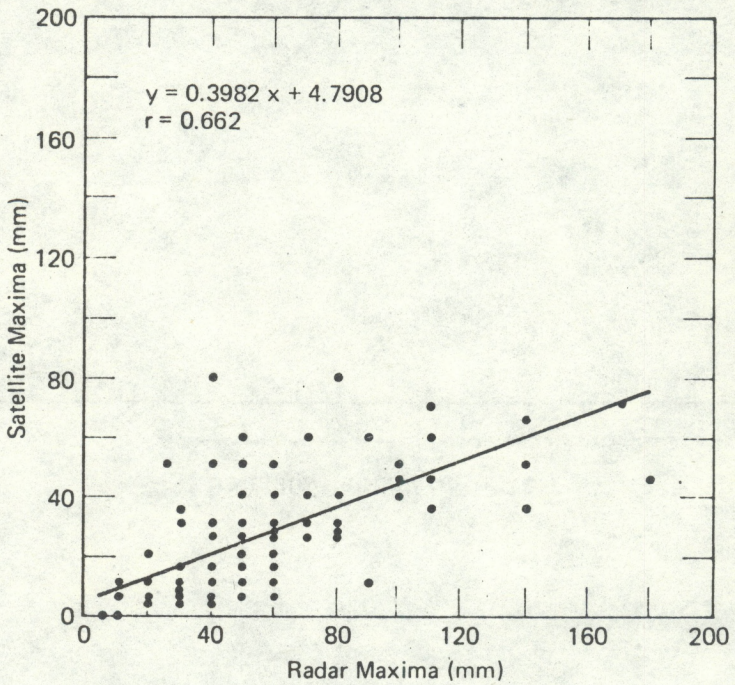

Figure 10. Scatter plot and regression of satellite versus radar maxima, daily for all phases, over the 3° square.

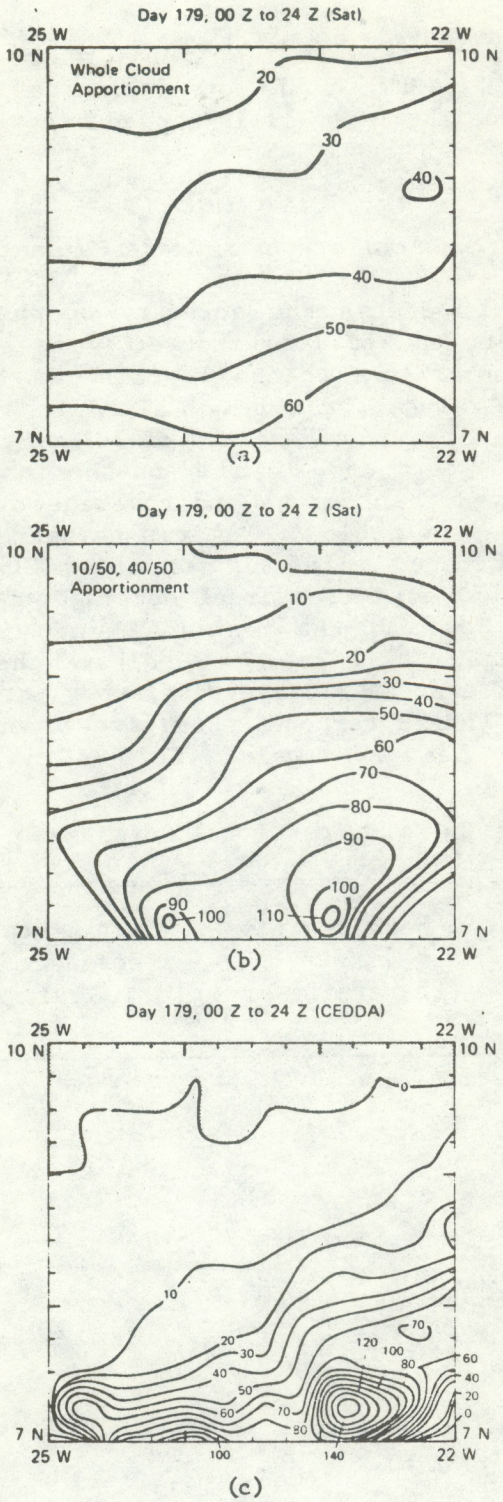

Figure 11. Comparison of radar-rain map and two satellite rain mapping schemes. Note the improvement with the 10-50/40-50 apportionment scheme.

According to Gray (1977) the GATE mean zonal winds by phase were easterly, averaging 11 to 14 m s^{-1}. Such conditions would readily account for the westward displacement, since the rainfall is mapped according to cloud top temperature.

4.2 Accuracy of A-Scale Estimates

It is impossible to assess the accuracy of the A-scale rain estimates directly. An assessment can be made indirectly by extrapolating the B-scale radar and satellite comparisons to the A scale. A further check on the accuracy of the A-scale rainfall can be obtained by reference to the work of Gray (1973), who indicates that an average of 20% of the tropics receives rain daily and that a mean of 2.5 cm d^{-1} falls in these raining areas. The daily average satellite-derived rain amount and coverage over the A- and A/B-scale raining areas are listed in table 7. As can be seen, the mean areal coverage of daily satellite-estimated rainfall was about 20% in each phase, which agrees with Gray's (1973) estimated areal coverage of daily rainfall over the tropics as a whole. However, the mean GATE amounts are lower than Gray's overall tropical estimates by 1 cm d^{-1}. Perhaps the discrepancy can be explained by regional differences. Gray's estimates were based on western North Pacific Ocean and West Indies regions, which are convectively more active than the eastern Atlantic. Mean A/B-scale rainfalls over the raining areas are also included in table 7.

Table 7. Mean Rainfall in, and Fractional Coverage of, Satellite-Derived Rain Areas Over the A and A/B Scales

Period	Mean A-scale rain (in raining area) (cm d^{-1})	Mean A-scale coverage of rain (%)	Mean A/B-scale rain (in raining area) (cm d^{-1})
Phase I (Day 179-197)	1.41	20	1.33
Interphase (Day 198-208)	1.50	21	1.55
Phase 2 (Day 209-227	1.26	20	1.14
Interphase (Day 228-241)	1.58	19	1.74
Phase 3 (Day 242-262)	1.37	26	1.38
Phase 1, 2, 3	1.35	22	1.28
All GATE	1.41	22	1.40

Additional checks are possible. NASA scientists (Rao, Abbott, and Theon, 1976) produced a global rain atlas for 11 December 1972 to 28 February 1975 from Nimbus 5 microwave (ESMR) imagery. The atlas also included the GATE period, so it is natural to compare the ESMR estimates with ours. This was done for the areas shown in table 8 for all GATE. Examination of the results shows that the NASA/ESMR results are consistently low compared with the NHEML rainfall estimates by an average of about 50%. This difference is, in part, due to the disparate spatial resolutions of the Nimbus ESMR (nominally 25 km) and the SMS IR data (nominally 8 km in the raw data). Because the NHEML estimates are close to the combined rain gage and radar ground truth in phases 1 and 3, and low compared with this standard in phase 2, it appears that the NASA/ESMR atlas underestimates rainfall by at least 50% in the eastern Atlantic. Extrapolation of this result to other tropical areas may not be valid.

The A-scale satellite rainfall estimates for the three GATE phases were compared with rain gage measurements in Africa. The rain gage locations are shown in figure 12. Phase areal averages were computed in 2° latitude intervals for both the satellite and rain gage measurements beginning at 5° N and ending at 19° N. We obtained the rain gage area averages by summing the rain gage readings and dividing by the number of gages. No weighting as a function of gage density was applied. The mean satellite rainfalls were obtained from the computer output.

Results are presented in figure 13. In general, the satellite phase rainfalls agree with the rain gage measurements up to 11° N. North of this

Table 8. ESMR-NHEML GATE Rainfall (mm h^{-1}) Comparisons

Region		NHEML	ESMR	Ratio
Area 1	47.5°W - 42.5°W 4°N - 8°N	0.14	0.06	2.33
Area 2	42.5°W - 37.5°W 4°N - 8°N	0.22	0.15	1.47
Area 3	32.5°W - 27.5°W 4°N - 8°N	0.29	0.29	1.00
Area 4	22.5°W - 17.5°W 4°N - 8°N	0.30	0.16	1.88
Area 5	27.5°W - 22.5°W 8°N - 12°N	0.24	0.13	1.85
Area 6	22.5°W - 17.5°W 8°N - 12°N	0.42	0.31	1.35
All		0.27	0.18	1.50

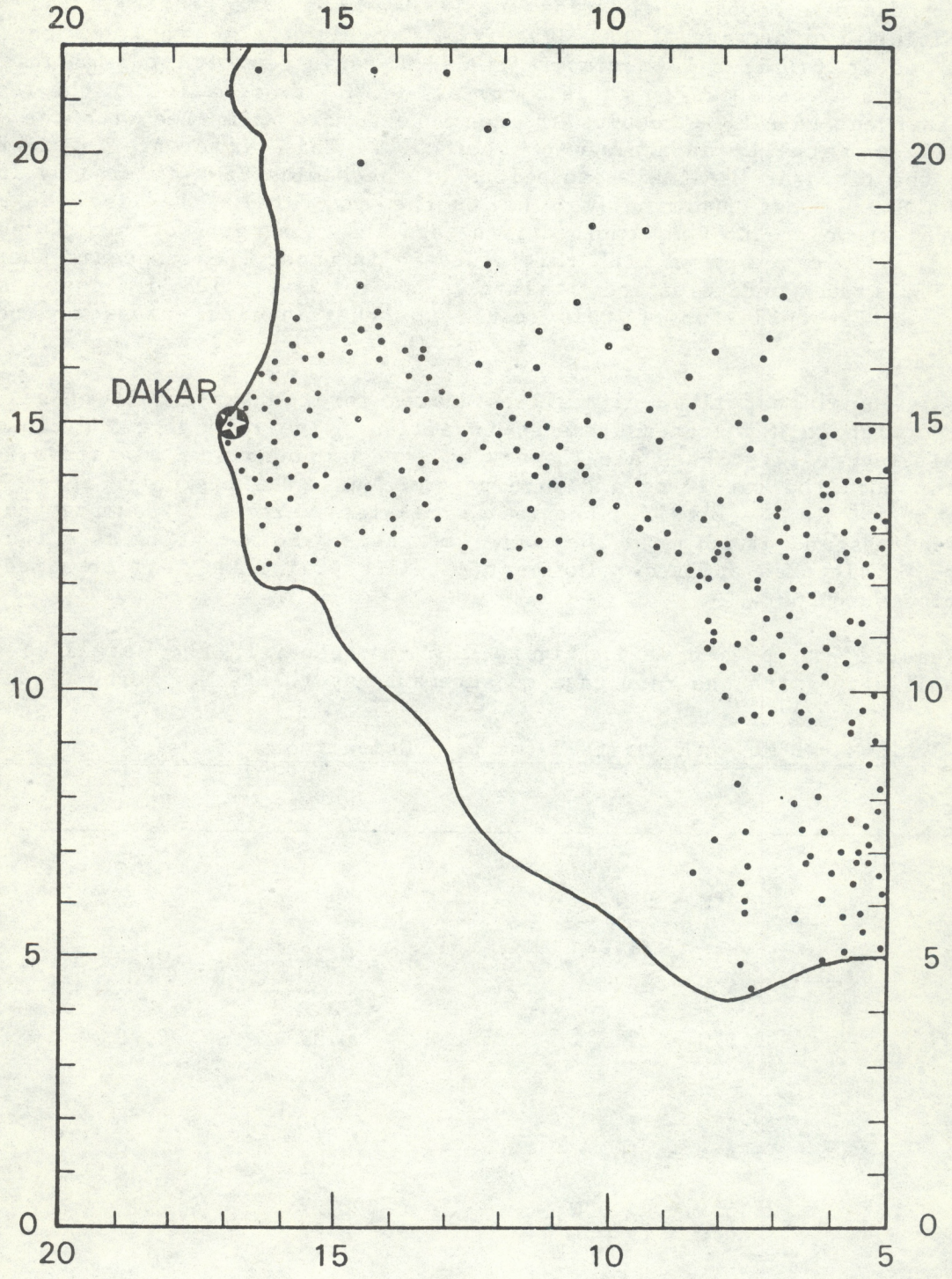

Figure 12. GATE rain gage locations in Africa.

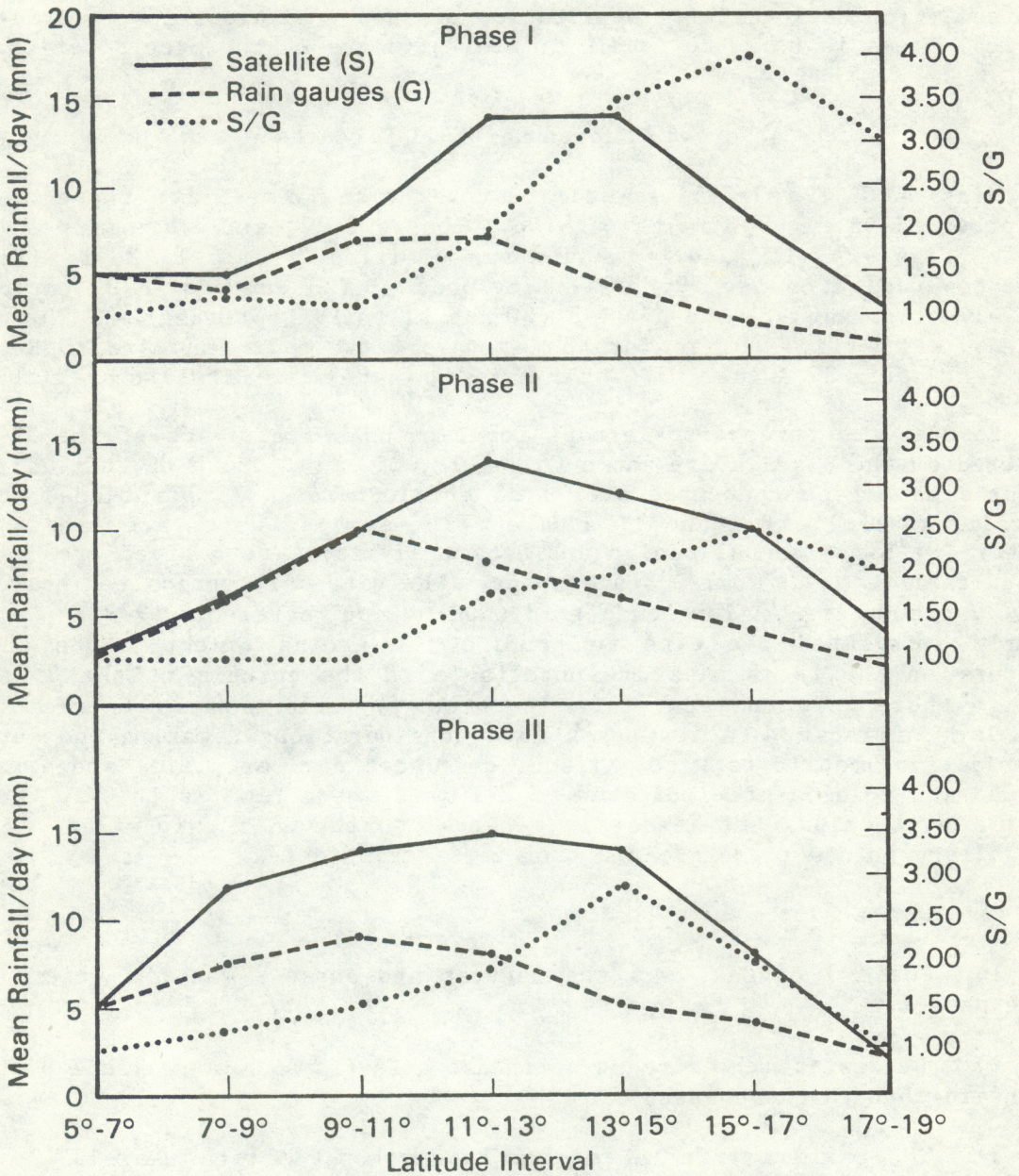

Figure 13. Comparison of satellite and rain gage areal average rainfall, by phase, in African triangle (20° N, 15° W; 20° N, 5° W; and 5° N, 5° W).

latitude in the more arid regions toward the Sahara, the satellite tends to overestimate the actual rainfall. This is understandable because the empirical relationships used to estimate rainfall in GATE were derived in a moist, tropical, Florida location. Application of these relationships to drier, non-tropical areas is bound to result in overestimates of the precipitation.

4.3 Mapped Rainfall Products

Maps of GATE rainfall accumulated over time frames of a phase or longer are provided in figures 14 through 18. Phases 1, 2, and 3 are mapped individually (figs. 14, 15, and 16). The map entitled "Phases 1, 2, 3" (fig. 17) indicates data from the 59 days during phase 1 (28 June to 16 July), phase 2 (28 July to 15 August) and phase 3 (30 August to 19 September). The map entitled "GATE" (fig. 18) is for the 85 days between 27 June and 20 September 1974 (excluding 22 August 1974, for which no satellite data are available).

Besides the three A-scale maps for each phase, blow-ups of the 3° square centered on the B scale are shown (figs. 19, 20, 21). Both of these satellite products have been contoured over 1/3° grid squares. Also included are maps of radar rainfalls for the 3° square. These maps, which are labeled CEDDA (Center for Experimental Design and Data Analysis), are derived from digital, C-band radar data on four B-scale ships. The data were composited hourly over a $\frac{1}{4}°$ latitude by $\frac{1}{4}°$ longitude grid (Hudlow and Patterson, 1979). We subsequently integrated the data to produce the ground truth. Note that the contours on the radar maps are unreliable in the corners of the 3° square, because there were no radar data in three $\frac{1}{4}°$ grid squares in each corner. This lack of radar data was taken into consideration in making the satellite and radar volumetric rain comparisons discussed earlier. Time and area integrated rain volumes are indicated on all maps where time is in GMT. For comparable daily maps, the reader is referred to the GATE rain atlas. Some of the salient points to be gleaned from these maps follow.

On the A scale:

1) Phase 3 of GATE was the wettest and phase 2 was the driest of the three phases.

2) The west-southwest/east-northeast axis of maximum rainfall progresses northward through the phases.

3) The maximum rainfall occurs in southwest Africa near 11° N in all phases; it amounts to over 1600 mm for all of GATE.

4) As documented earlier, one can have high confidence in the satellite-derived rain estimates for phases 1 and 3 and somewhat less confidence for phase 2.

5) The climatologically dry area in northeastern South America shows clearly on the A-scale rain maps.

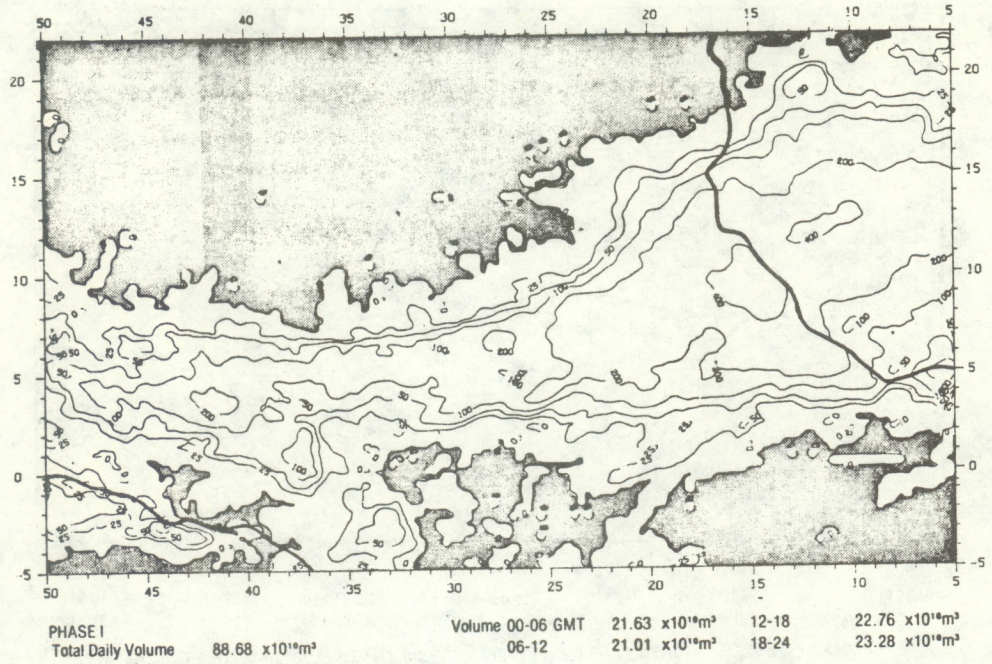

Figure 14. Mapped total rainfall (mm) for phase 1, based on whole-cloud apportionment.

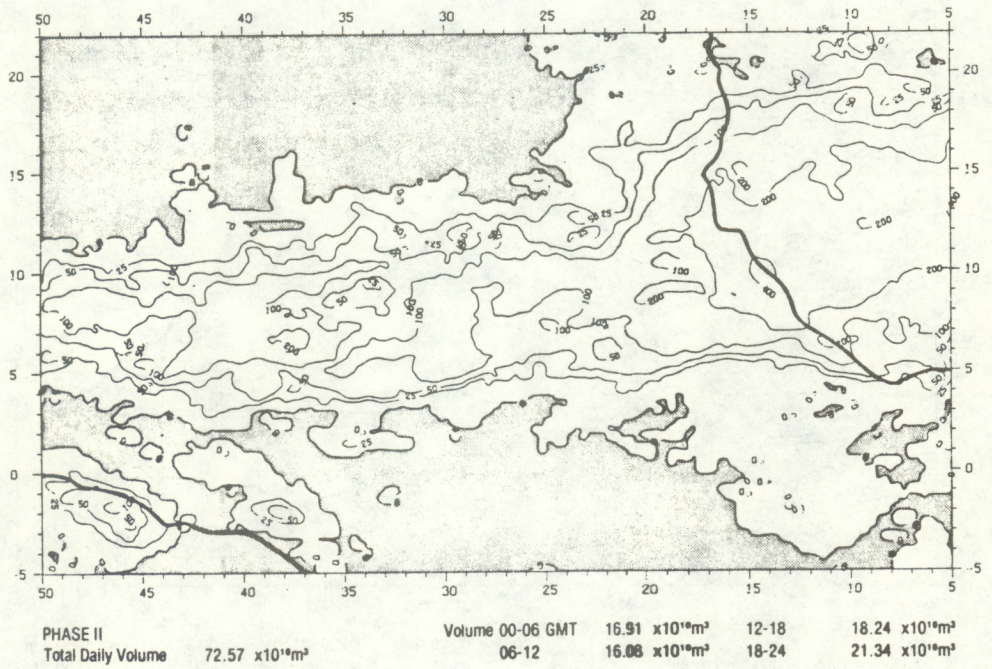

Figure 15. Mapped total rainfall (mm) for phase 2, based on whole-cloud apportionment.

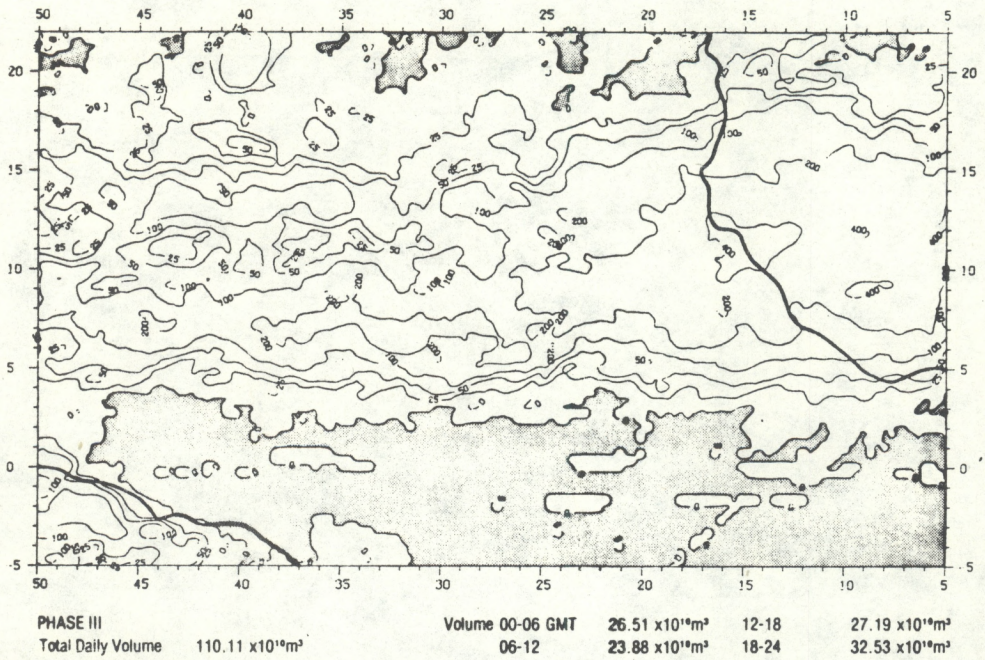

Figure 16. Mapped total rainfall (mm) for phase 3, based on whole-cloud apportionment.

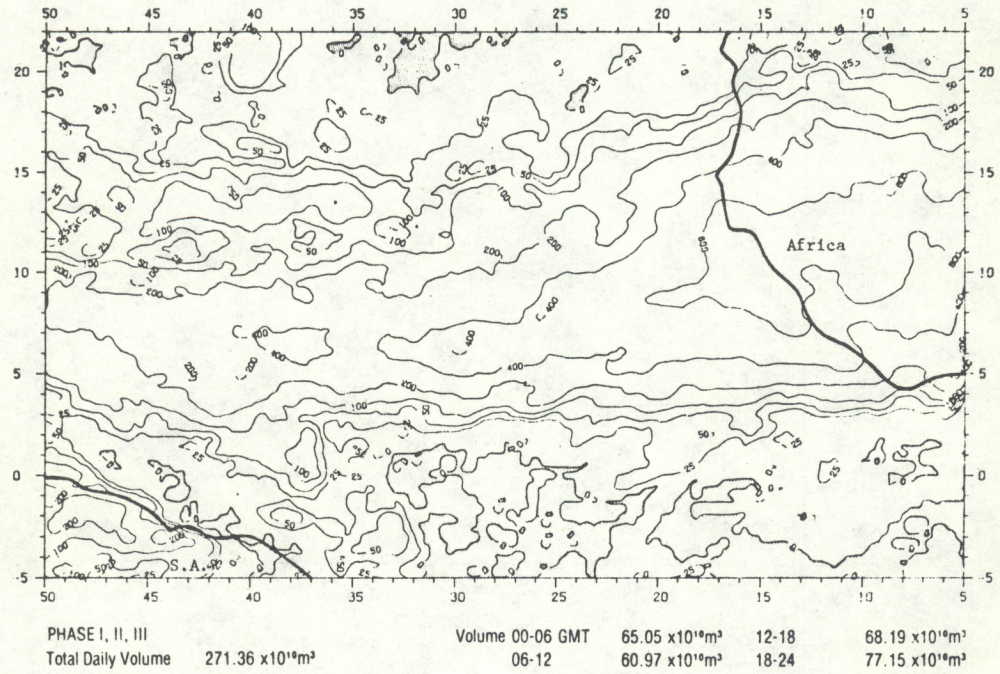

Figure 17. Mapped total rainfall (mm) for all phases, based on whole-cloud apportionment.

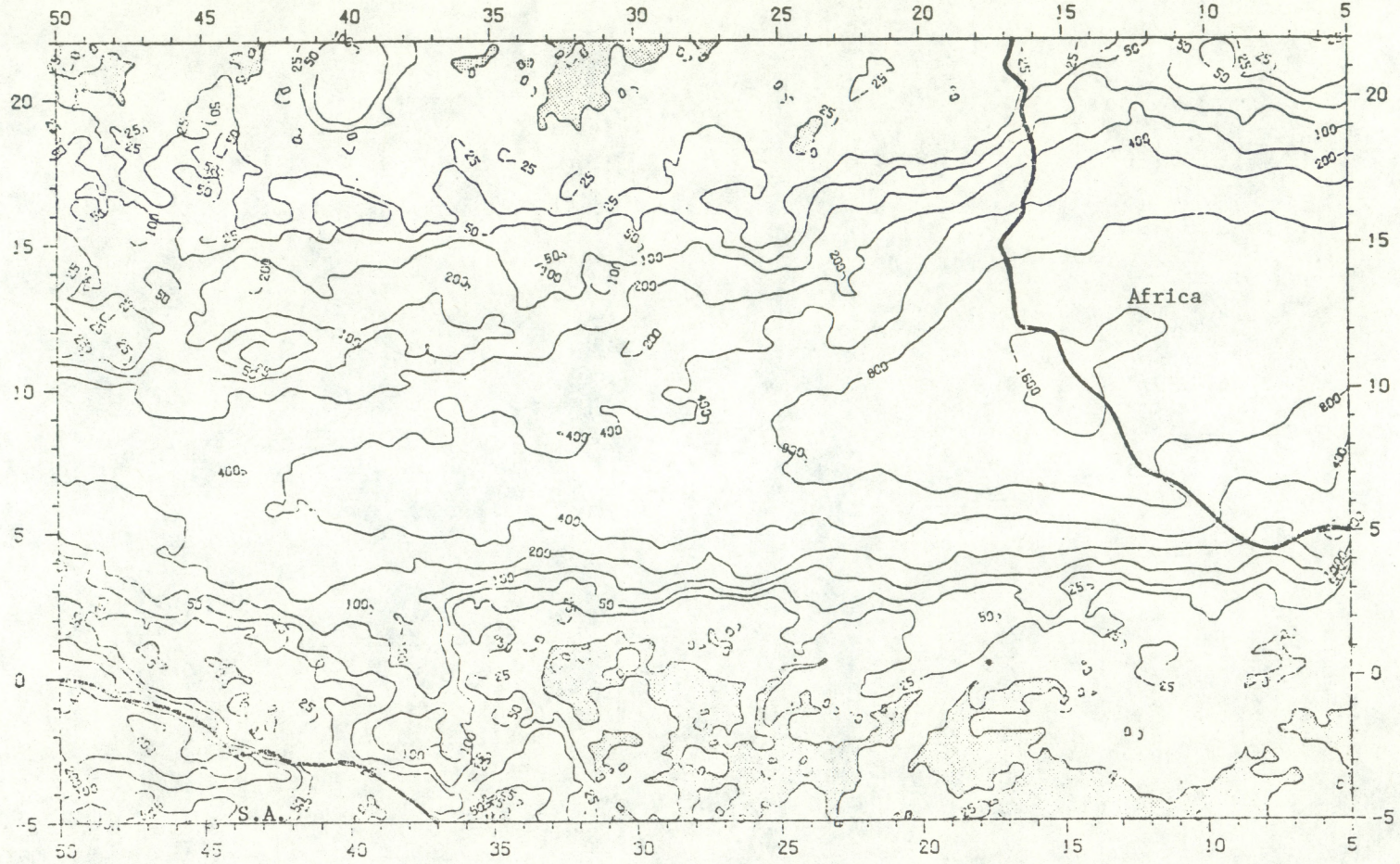

Figure 18. Mapped total rainfall (mm) for all GATE (27 June to 20 September 1974, excluding 22 August).

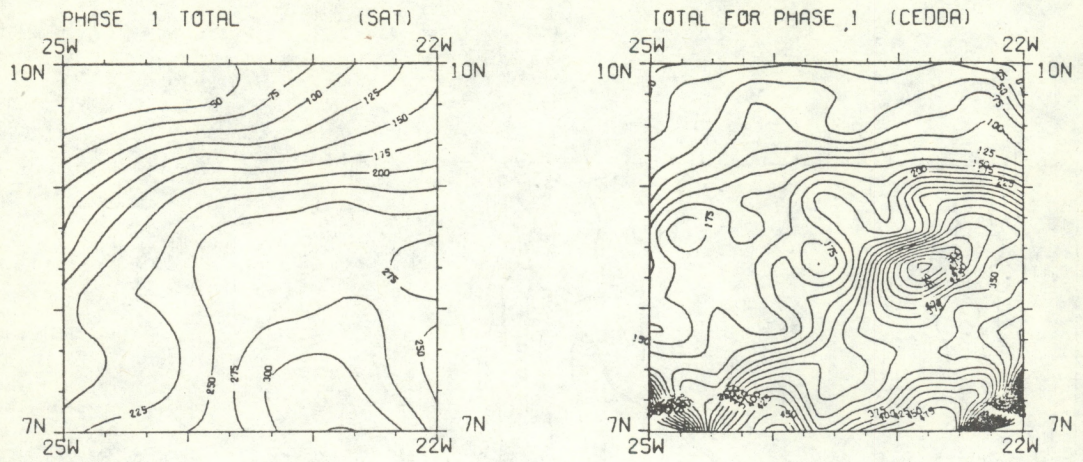

SATELLITE		PHASE I	RADAR	
Total Daily Volume	200.98 x10⁸m³	RATIO	Total Daily Volume	218.63 x10⁸m³
Volume 00-06 GMT	32.64 x10⁸m³	R/S = 1.09	Volume 00-06 GMT	37.37 x10⁸m³
06-12	35.16 x10⁸m³		06-12	49.14 x10⁸m³
12-18	79.96 x10⁸m³		12-18	76.52 x10⁸m³
18-24	53.22 x10⁸m³		18-24	55.62 x10⁸m³

Figure 19. Comparison of mapped satellite and radar rainfall for phase 1 over the 3° square.

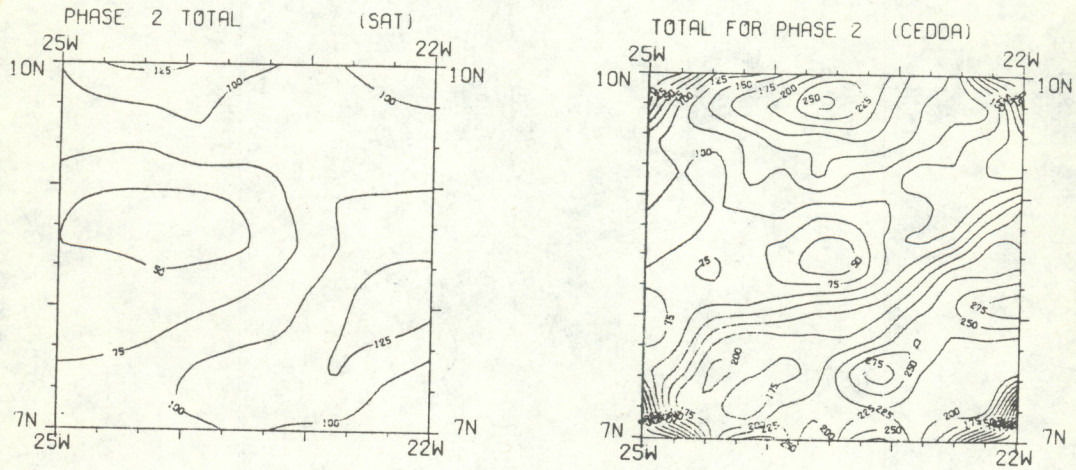

SATELLITE		PHASE II	RADAR	
Total Daily Volume	89.78 x10⁸m³	RATIO	Total Daily Volume	155.15 x10⁸m³
Volume 00-06 GMT	15.02 x10⁸m³	R/S = 1.73	Volume 00-06 GMT	35.57 x10⁸m³
06-12	30.86 x10⁸m³		06-12	51.64 x10⁸m³
12-18	25.52 x10⁸m³		12-18	36.14 x10⁸m³
18-24	18.38 x10⁸m³		18-24	31.68 x10⁸m³

Figure 20. Comparison of mapped satellite and radar rainfall for phase 2 over the 3° square.

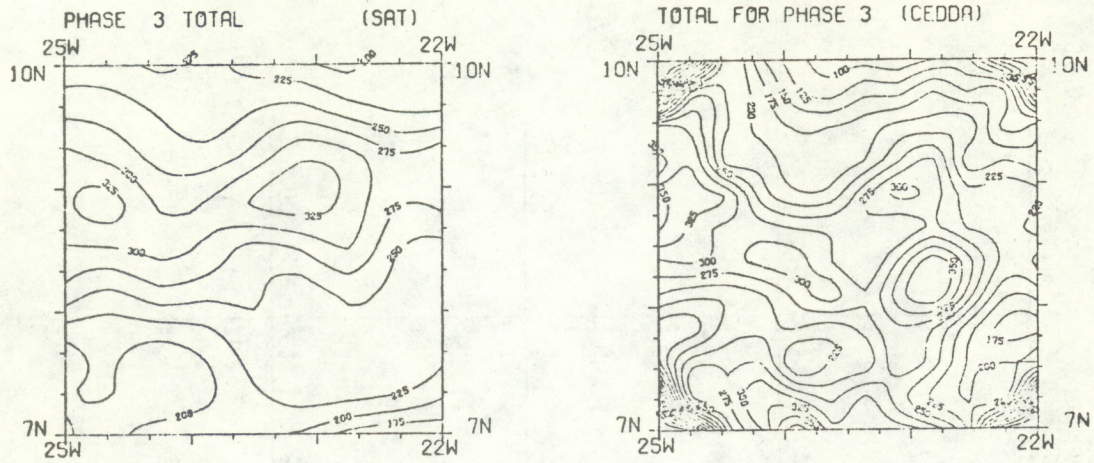

Figure 21. Comparison of mapped satellite and radar rainfall for phase 3 over the 3° square.

Over the 3° square (where, again, the contours in the corners of the radar depictions are fictitious because of a lack of data):

1) The patterns of rainfall derived from the satellite imagery are similar to those obtained from the shipboard radars, but the maxima are higher and the detail is greater in the radar depictions. The reasons for this difference are discussed in section 4.1.

2) The magnitude of the satellite and radar estimates of phase rainfall agree rather well for phases 1 and 3, but the satellite estimates are low compared with the radar for phase 2. This finding is treated in section 4.1.

4.4 Longitudinal Rainfall Slices

Longitudinal slices showing the north-south variation of rainfall between 5° S and 22° N over western Africa (10° W), the center of the B array (23.5° W) and two midocean locations (30° W and 40° W) are shown in figure 22 for each phase, all phases combined, and all GATE. Note that the axis of maximum rainfall typically slopes west-southwestward from Africa to 40° W and that the maximum rainfall occurs along 10° W longitude and the minimum occurs along 40° W longitude.

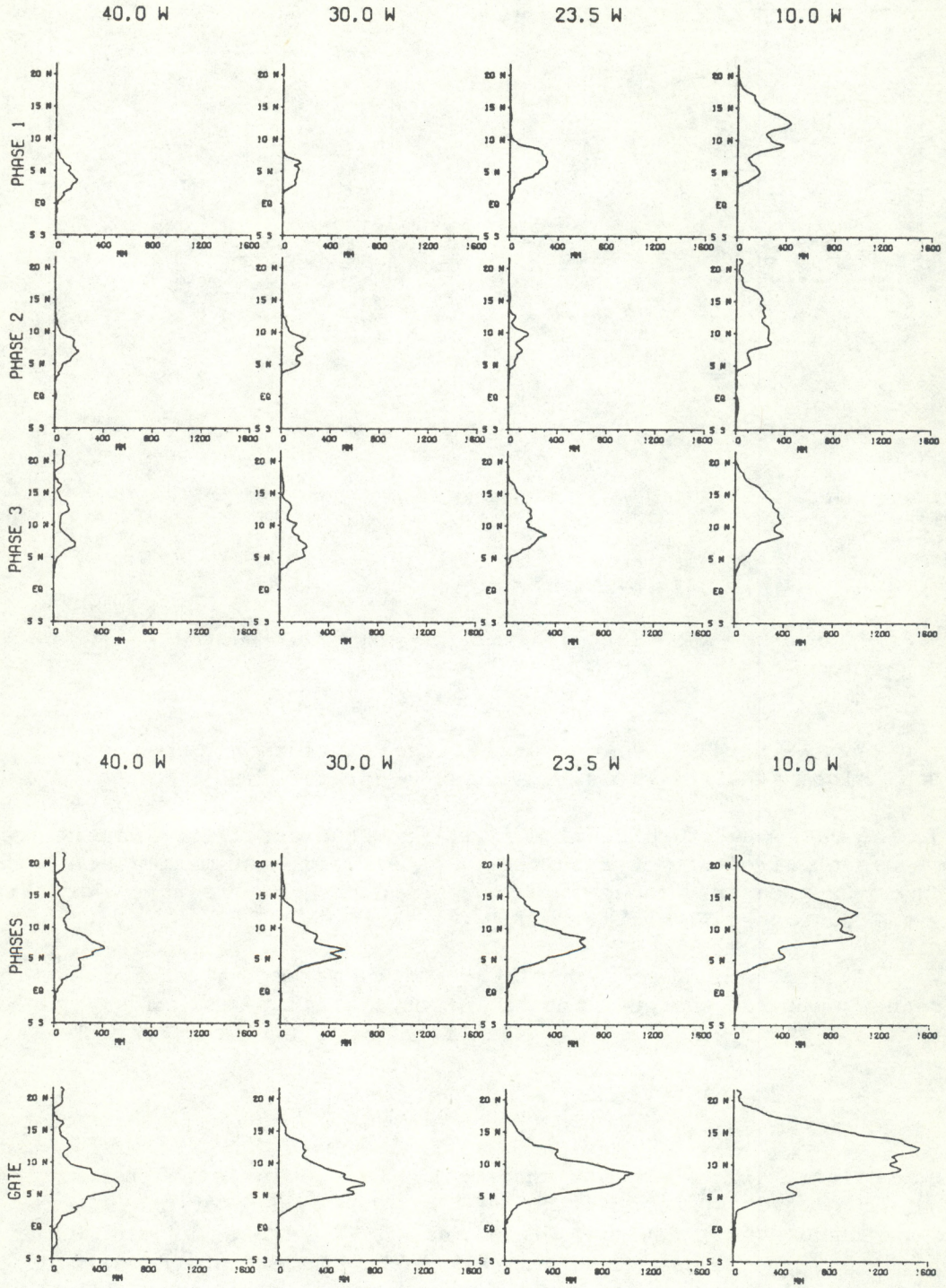

Figure 22. Longitudinal slices of satellite rainfall between 5° S and 22° N over four locations for each phase, all phases, and all GATE.

4.5 GATE Rainfall and Sea Surface Temperature

Superposition of the mean sea surface temperature analyses by Krishnamurti et al. (1976) for the phases of GATE onto the satellite-derived A-scale rainfall analyses (figs. 23, 24, 25) produced some interesting results. There appears to be a relationship between sea surface temperature and rainfall; the rain maxima move northward with the sea surface temperature maxima. Almost all of the significant phase rainfall occurs over oceanic regions warmer than 26° C.

4.6 Diurnal Variation of Rainfall in GATE

Dirunal rainfall variability is treated extensively in the rain atlas; selected products are shown here. The diurnal rainfall inferences were made on the basis of rain amount rather than rain frequency. The time of the day having the most rain, and not the most occurrences of rain, is the time of rain maximum.

The period of the day having the most rainfall can be inferred from figures 26 through 31 for the three GATE phases, for all phases, and for all GATE. The numbers on each map refer to the 6-hr period of the day having the maximum rainfall. Number 1 is 00 to 06 GMT, 2 is 06 to 12 GMT, 3 is 12 to 18 GMT and 4 is 18 to 00 GMT. Areas having numbers 1 or 4 are stippled on the map. There is a clear tendency for the maximum rainfall to occur in periods 1 and 4 in Africa and South America and in periods 2 and 3 over the eastern Atlantic. This implies a nocturnal rainfall maximum over the land areas and a daytime maximum over the water areas. The inferred percentages of the daily rainfall that fell in the four 6-hr periods are in the atlas. A summary of our results and those of other GATE investigators is in table 9. Note that our results for the 3° square and the A/B scale and those of Hudlow (1977) for the master array indicate a distinct maximum of rainfall in the period 12 to 18 GMT for all phases of GATE with 30 to 35% of the daily B-scale rainfall falling in this period. The budget study by Dewart (1978) for the A/B scale suggests a flat maximum of rainfall in the period 06 to 12 GMT with 29% of the daily precipitation as compared to 27% for the period 12 to 18 GMT.

4.7 Number of Cloud Growths, Mergers, and Dissipations, and Their Diurnal Variability

Maps of the number of occurrences in GATE of cloud growths, mergers, and dissipations, and their diurnal variability over the A scale are included in the rain atlas. A cloud merger is defined as the joining of two formerly independent convective entities at the 253° K threshold. New cloud growths and dissipations are defined as the appearance and disappearance of cloud entities at this threshold. Examination of the many maps revealed that most of the new growths and dissipations occurred within the region of maximum rainfall and there was an obvious tendency for more cloud mergers near the southwest coast of Africa in the region of maximum rainfall as shown in figure 31. The numbers on this map are the number of cloud mergers within a 1° square during all GATE.

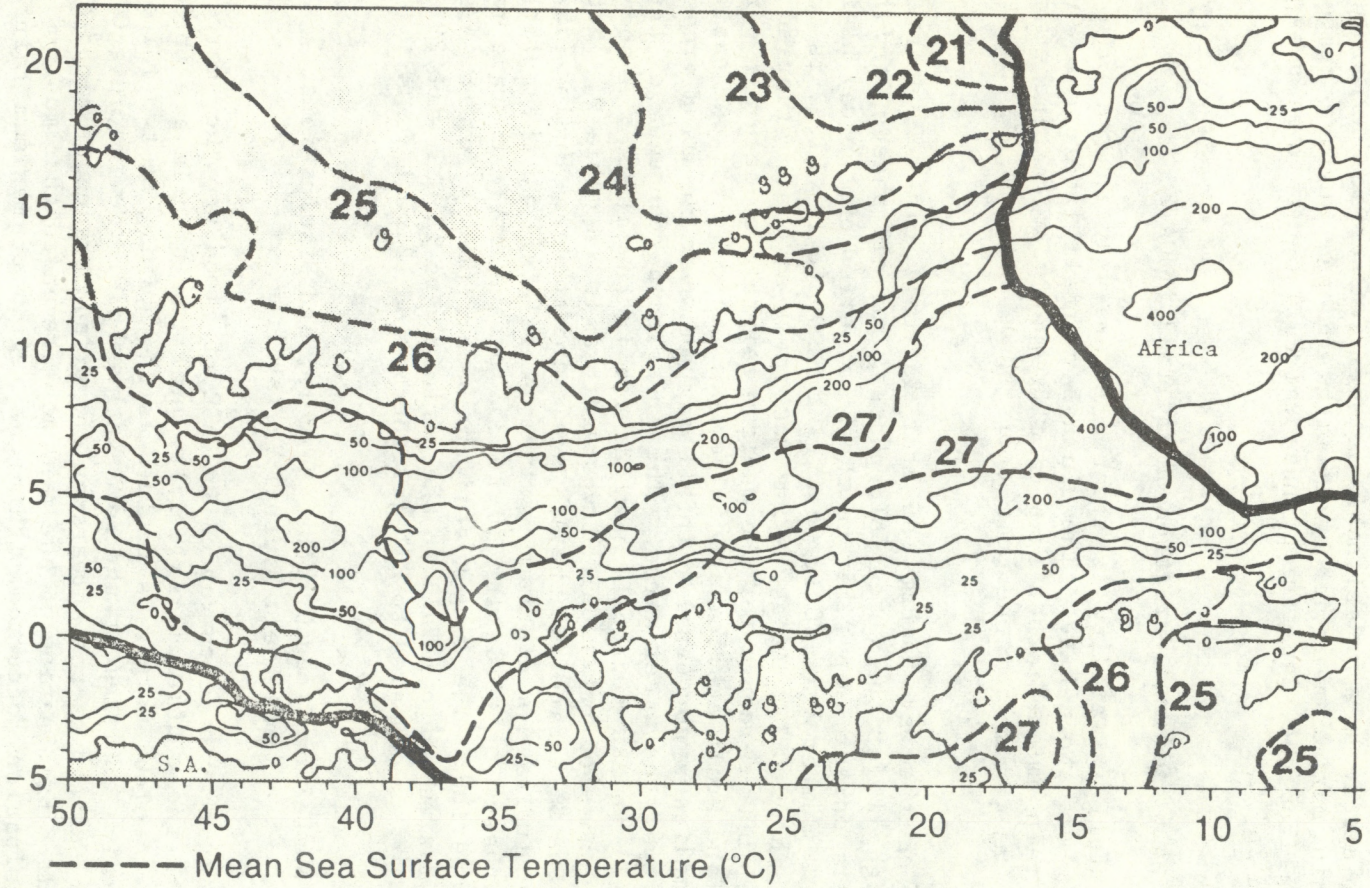

Figure 23. Superposition of the mean sea surface temperatures onto the satellite rainfall (mm) for phase 1 over the A scale (from Krishnamurti et al., 1976).

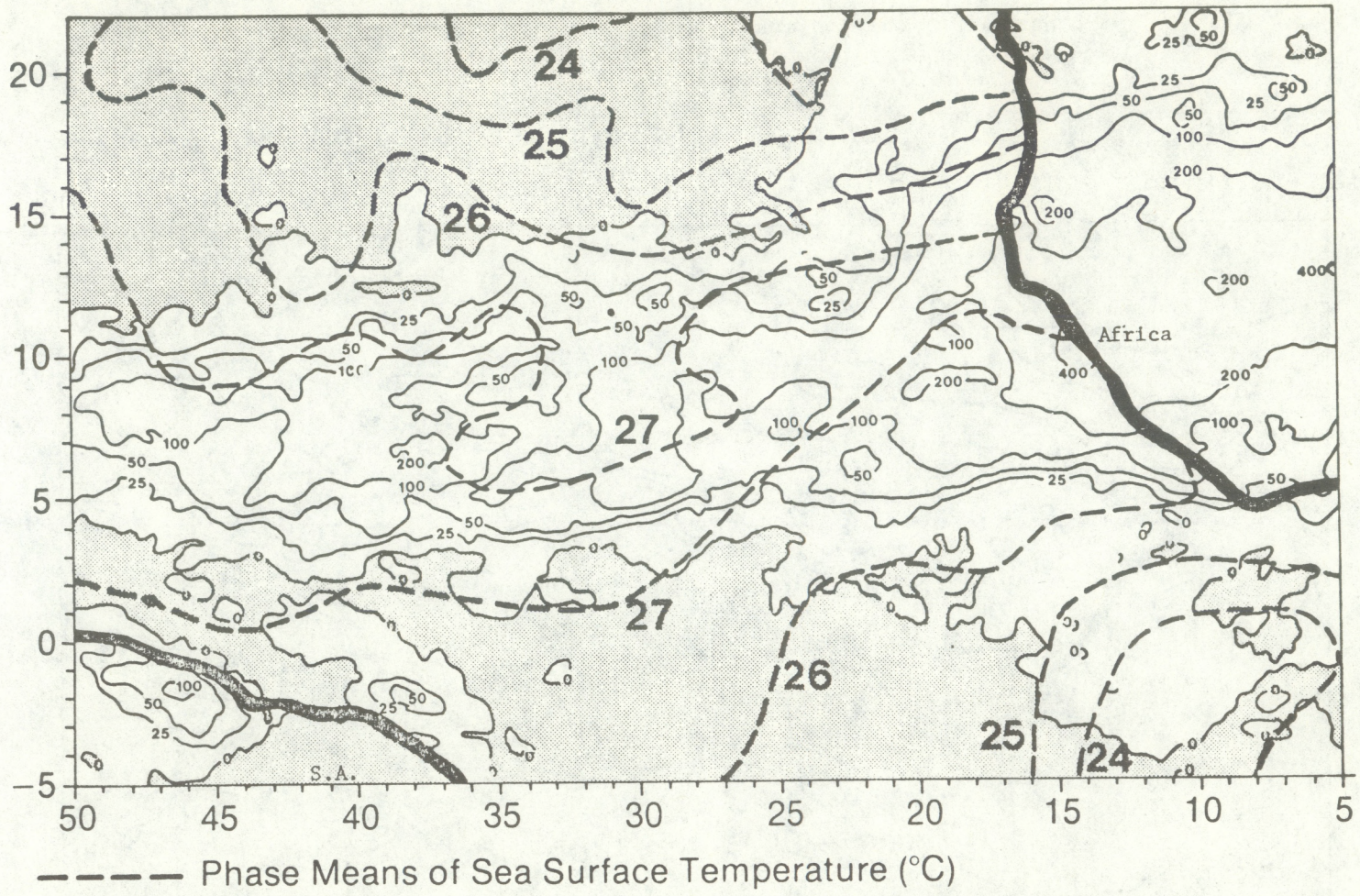

Figure 24. Superposition of the mean sea surface temperatures onto the satellite rainfall (mm) for phase 2 over the A scale (from Krishnamurti et al., 1976).

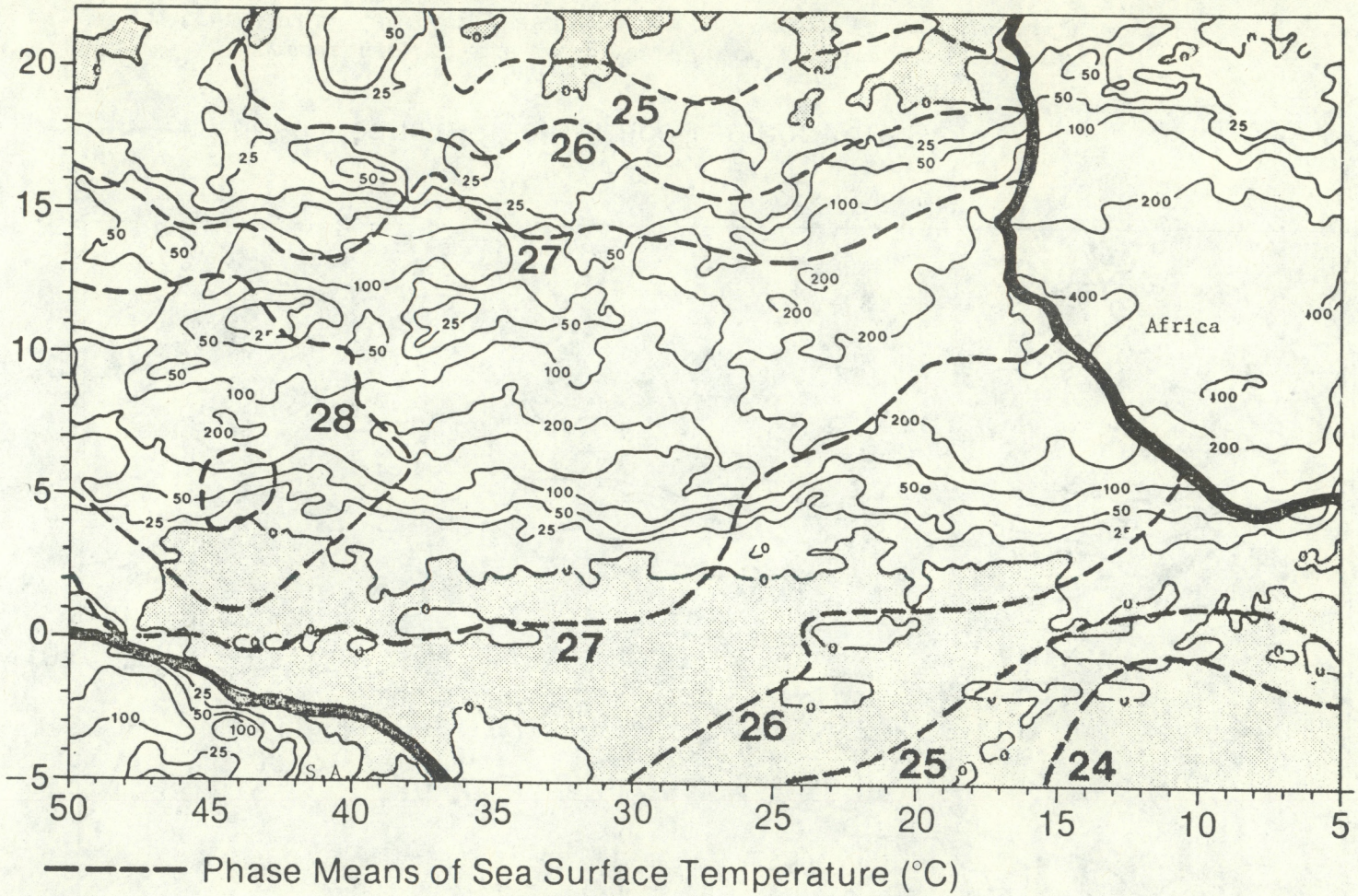

Figure 25. Superposition of the mean sea surface temperature onto the satellite rainfall (mm) for phase 3 over the A scale (from Krishnamurti et al., 1976).

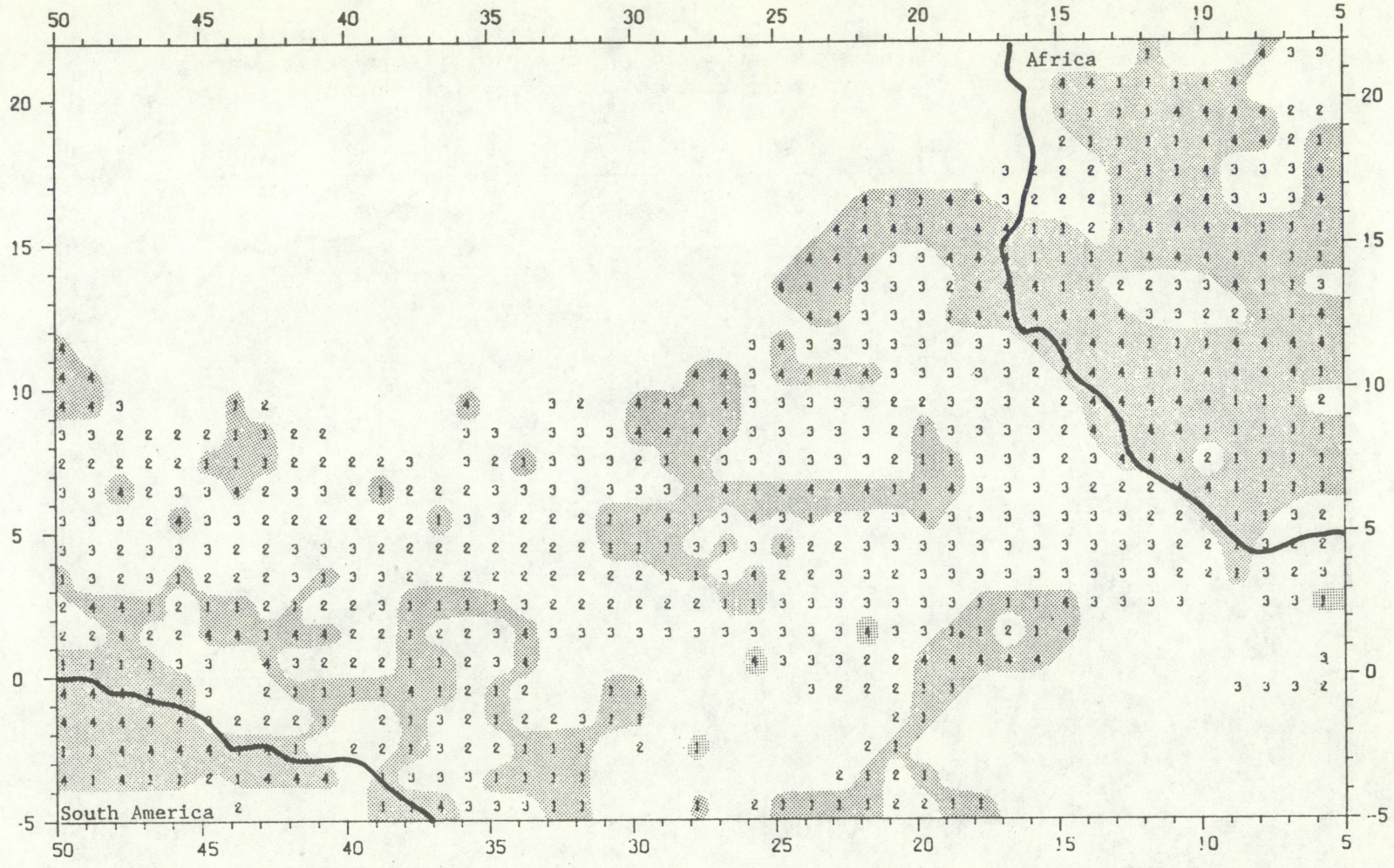

Figure 26. Diurnal variability of maximum rainfall for phase 1 over the A scale. The number 1 refers to 00 to 06 GMT, 2 is 06 to 12 GMT, 3 is 12 to 18 GMT, and 4 is 18 to 24 GMT.

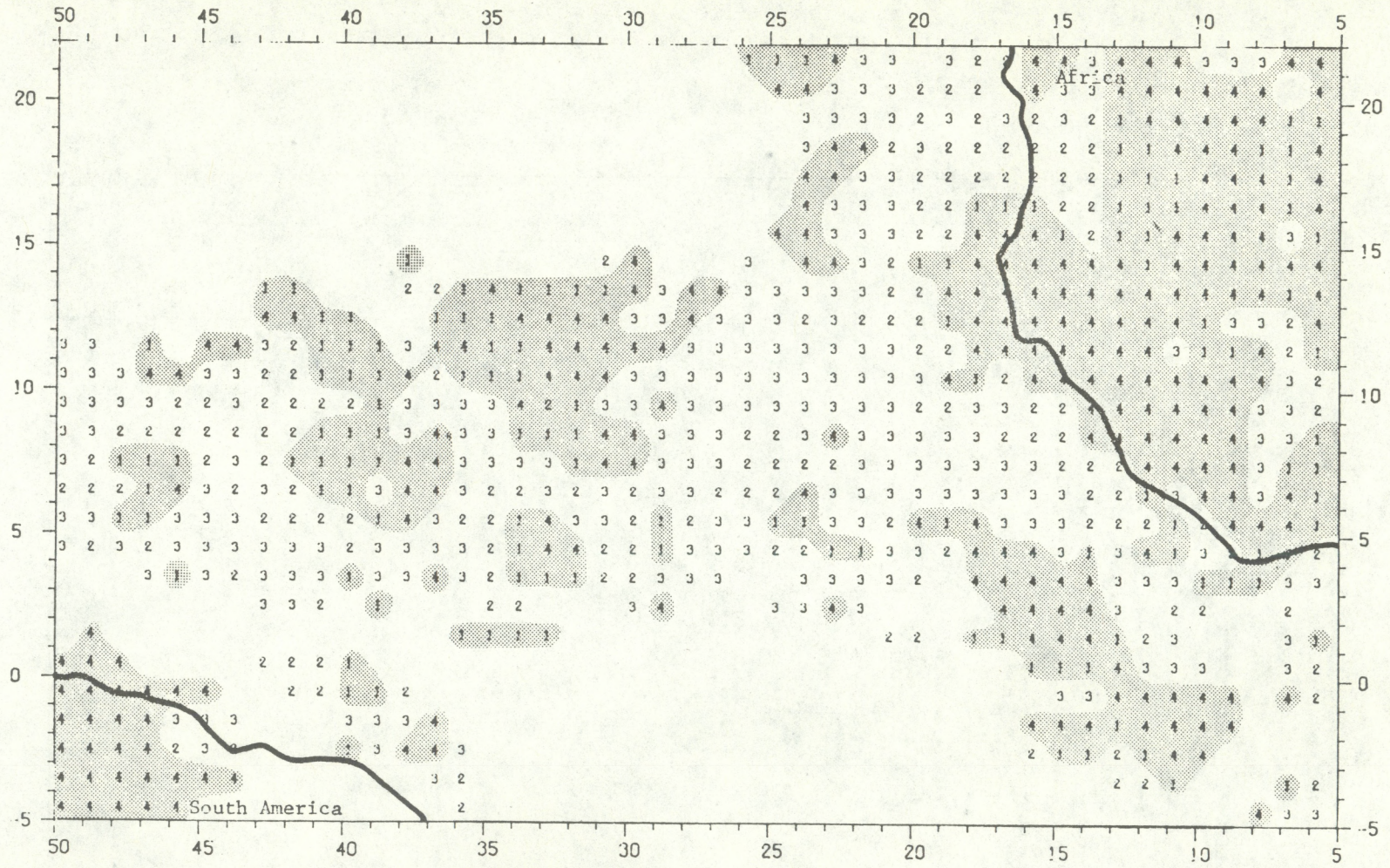

Figure 27. Diurnal variability of maximum rainfall for phase 2 over the A scale. The number 1 refers to 00 to 06 GMT, 2 is 06 to 12 GMT, 3 is 12 to 18 GMT, and 4 is 18 to 24 GMT.

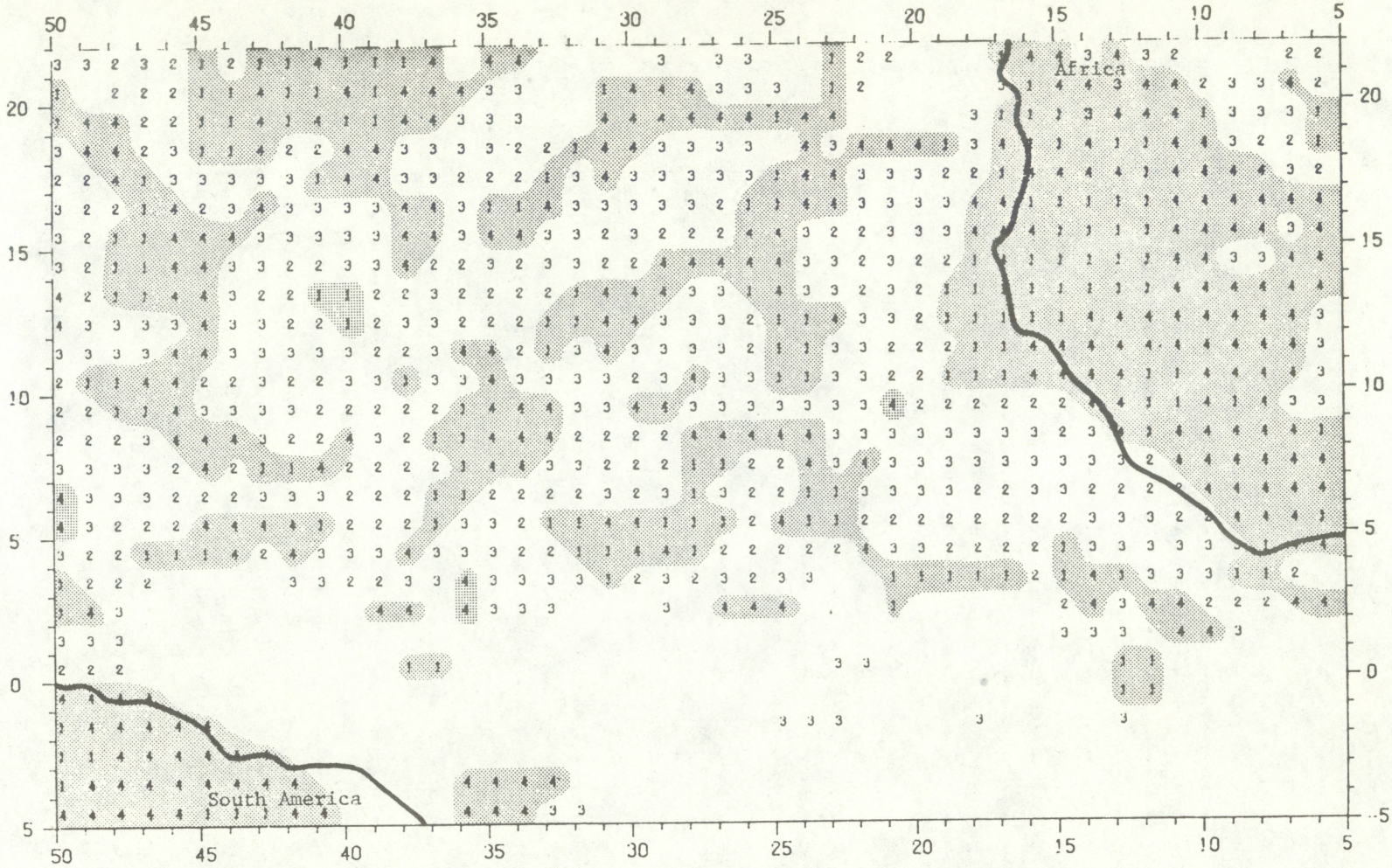

Figure 28. Diurnal variability of maximum rainfall for phase 3 over the A scale. The number 1 refers to 00 to 06 GMT, 2 is 06 to 12 GMT, 3 is 12 to 18 GMT, and 4 is 18 to 24 GMT.

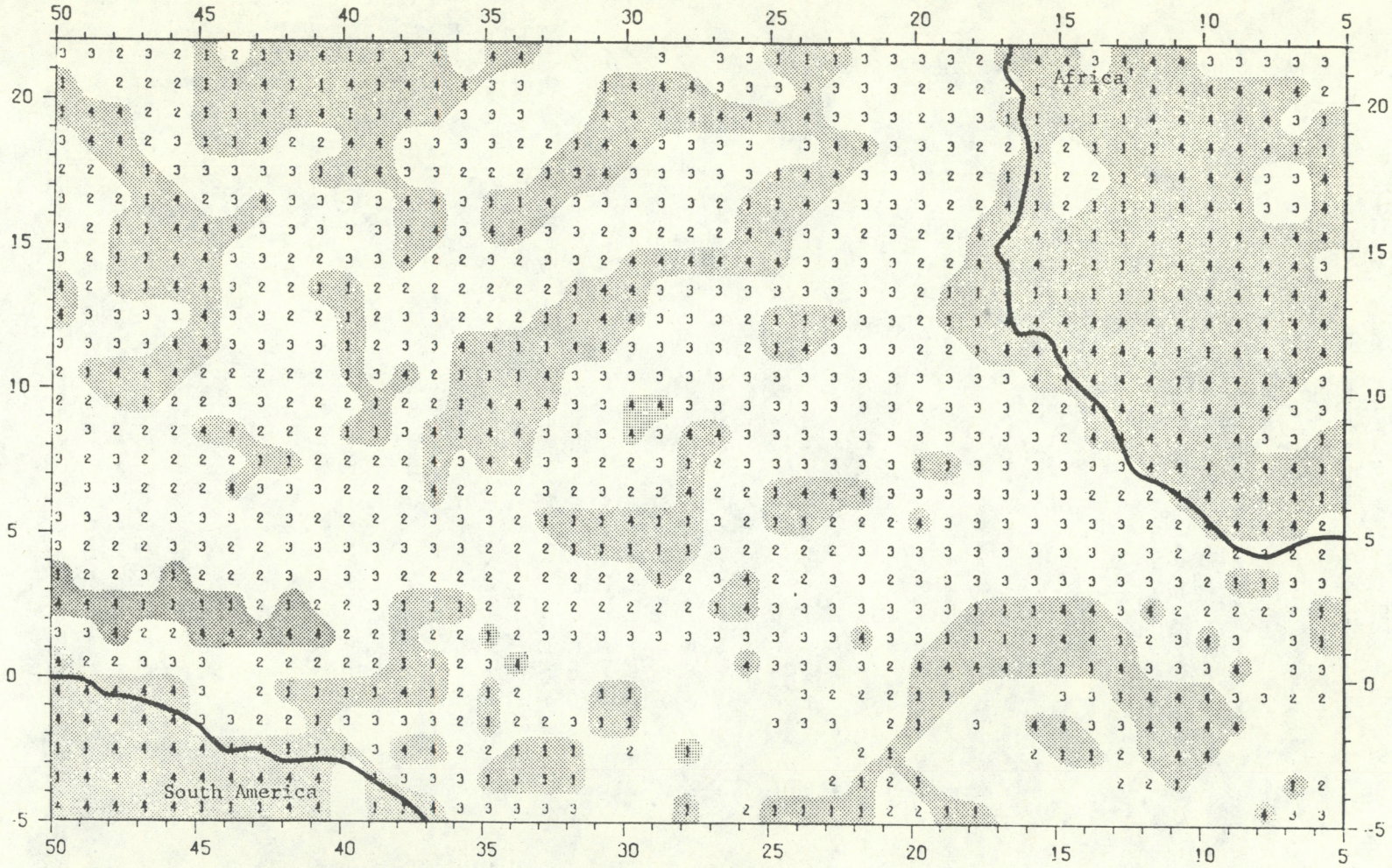

Figure 29. Diurnal variability of maximum rainfall for all phases over the A scale. The number 1 refers to 00 to 06 GMT, 2 is 06 to 12 GMT, 3 is 12 to 18 GMT, and 4 is 18 to 24 GMT.

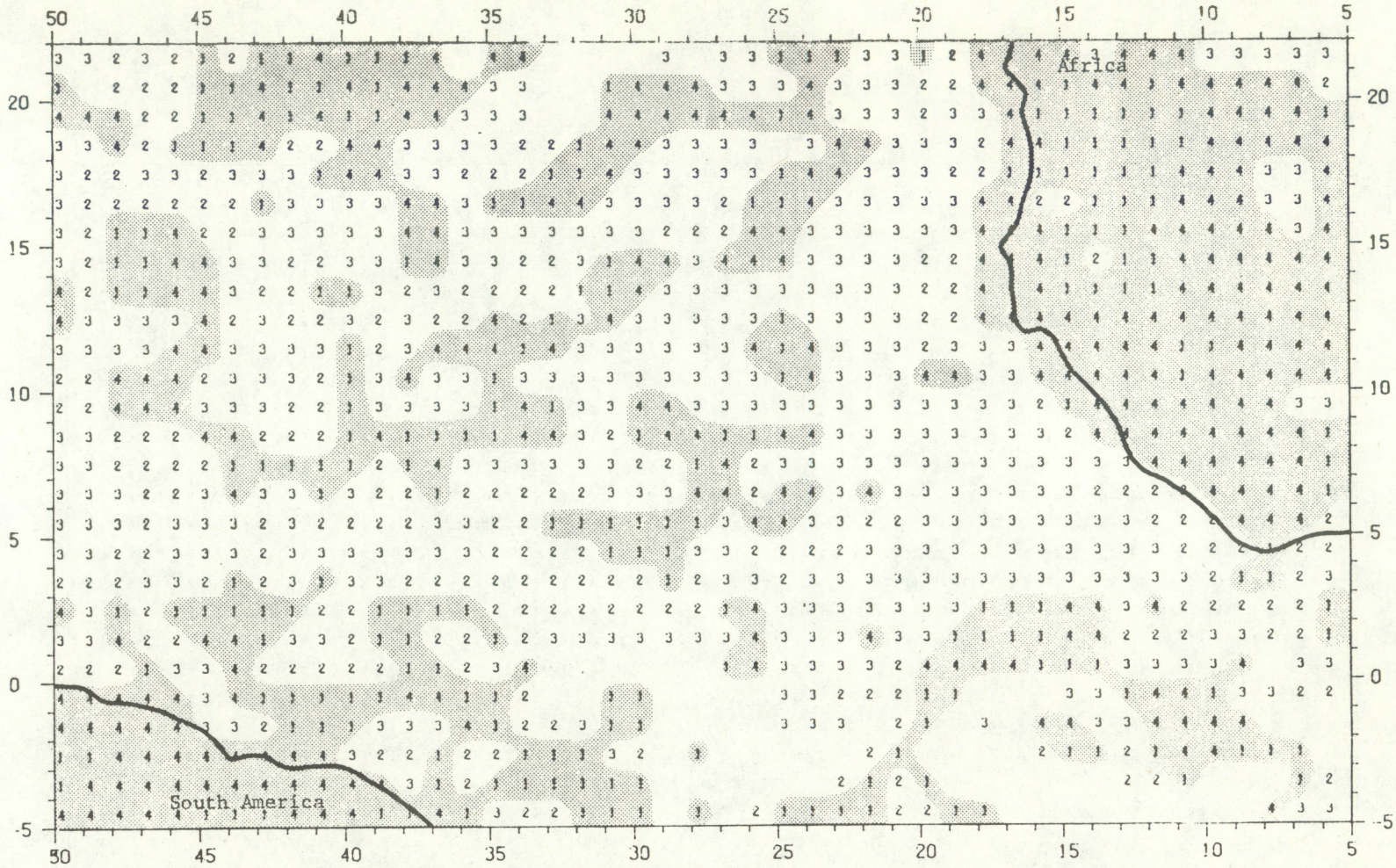

Figure 30. Diurnal variability of maximum rainfall for all GATE over the A scale. The number 1 refers to 00 to 06 GMT, 2 is 06 to 12 GMT, 3 is 12 to 18 GMT, and 4 is 18 to 24 GMT.

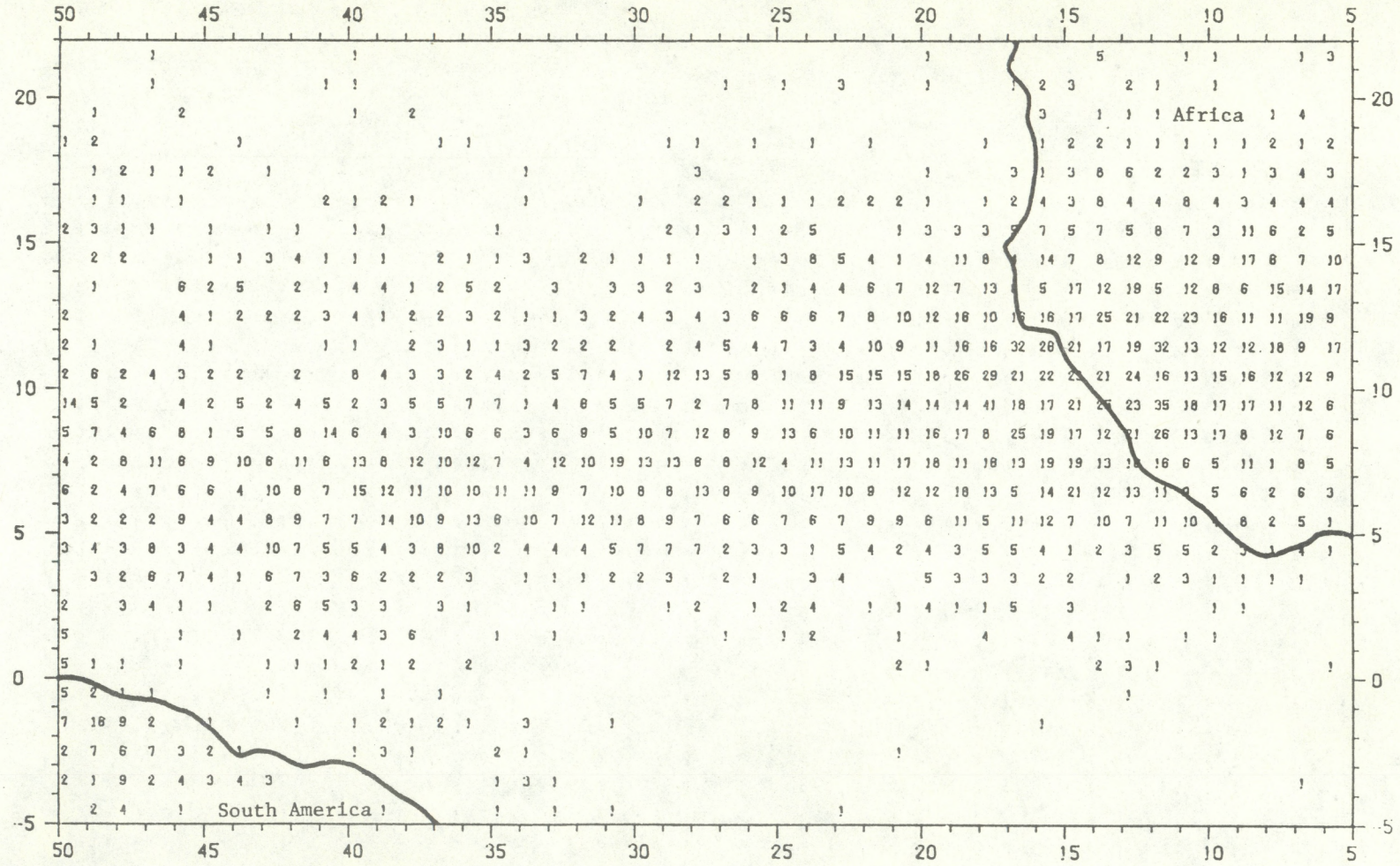

Figure 31. Number of mergers in all GATE. Resolution is 1° x 1° square.

Table 9. Diurnal Variation of GATE Precipitation

Period (GMT)	Griffith et al. (1979) for 3° square (satellite)		Hudlow (1977) for 3° square (radar)		Dewart (1978) for A/B scale (budget study)		Griffith et al. (1979) for A/B scale (satellite)
	Amount (cm d^{-1})	% of daily total	Amount (cm d^{-1})	% of daily total	Amount (cm d^{-1})	% of daily total	% of daily total
00 - 06	0.68	19	.86	20	1.39	23	20
06 - 12	0.75	21	1.04	25	1.76	29	22
12 - 18	1.19	34	1.24	31	1.64	27	33
18 - 24	0.90	26	1.02	24	1.27	21	25
00 - 24	0.88	--	1.04	--	1.53	--	--

The maps of the diurnal variability of cloud growths, mergers, and dissipations are not particularly informative. No diurnal preference for any of these cloud behavior parameters could be detected, except over the north part of South America where mergers were most likely between 18 and 00 GMT.

5. CONCLUSIONS

An automated technique that is based upon geosynchronous, infrared satellite imagery and a set of empirical relationships has been employed to estimate rainfall in the eastern Atlantic and western Africa during the GATE program. When compared with radar and rain gage estimates of precipitation, the satellite-derived rain estimates are low for the Atlantic and high for the African continent. Differences for the GATE master array are about 10% for phases 1 and 3, but about 70% for phase 2. The larger phase 2 disparity remains a matter for speculation, but it apparently does not carry over to the A scale. The daily satellite-derived maps of rainfall are generally similar to the radar products, but have lower point maxima. This difference is the result of the method of rainfall apportionment.

Based upon the satellite-derived rain estimates in GATE, the rainfall in the eastern Atlantic appears to be of lesser magnitude, but about equivalent in coverage to the western Pacific. This disparity is least near the southwest African coast near 11° N. Most of the significant convection activity occurs in the ITCZ stretching west-southwest from Africa. The rain maxima show a close association with the sea surface temperature. Ninety-five percent of the rainfall is contained within the 26° sea surface temperature envelope in all phases. A disproportionate amount of the rainfall occurs over the water areas during the day and over the land areas (Africa and the north part of South America) during the late evening.

6. ACKNOWLEDGMENTS

We are most grateful to W. Murray and to his predecessor, J. Rasmussen, of the NOAA GATE Office, for financial support and encouragement throughout the course of this research. R. Burpee provided the African rain gage observations and also made many helpful suggestions. The contributions of our colleagues D. Martin, D. Sikdar, and J. Stout at the University of Wisconsin, and J. Augustine and S. Browner of NOAA/ERL, are also appreciated. M. Hudlow was most helpful in the discussion of his radar products.

7. REFERENCES

Dewart, J. M. (1978): Diurnal variability in the GATE region. Atmospheric Science Paper No. 298, Colorado State Univ., Ft. Collins, Colo., 80 pp.

Gray, W. M. (1973): Cumulus convection and larger scale circulations I. Broadscale and mesoscale considerations. *Mon. Wea. Rev.*, 101:839.

Gray, W. M. (1977): Tropospheric mean state and variability; mean state and typical conditions. Report of the U.S. GATE Central Program Workshop, 25 July - 12 August, 1977, GATE Project Office, Rockville, MD, 199-213.

Griffith, C. G., W. L. Woodley, J. S. Griffin and S. C. Stromatt (1979): Satellite-Derived Precipitation Atlas for the GARP Atlantic Tropical Experiment. NOAA Atlas Series, Division of Public Documents, U.S. Government Printing Office, Washington, D.C.

Griffith, C. G., W. L. Woodley, P. G. Grube, D. W. Martin, J. Stout and D. N. Sikdar (1978): Rain estimation from geosynchronous satellite imagery--visible and infrared studies. *Mon. Wea. Rev.*, 106:1153.

Hudlow, M. D. (1977): Precipitation climatology for the three phases of GATE. Preprints, Second Conf. on Hydrometeor.-AMS, Boston, Mass., 290-297.

Hudlow, M. D. (1979): Mean rainfall patterns for the three phases of GATE Submitted to *J. Appl. Meteor.*

Hudlow, M. D., and V. Patterson (1979): GATE Radar Rainfall Atlas. NOAA Special Report EDIS Center for Environmental Assessment Services, Stock No. 003-019-00046-2, U.S. Gov't. Printing Office, Washington, D. C., 155 pp.

Hudlow, M. D., R. Arkell, V. Patterson, P. Pytlowany, F. Richards and S. Geotis (1979): Calibration and intercomparison of the GATE C-band radars. NOAA Tech. Memo. EDIS-31, Center for Environmental Assessment Services, U. S. Gov't. Printing Office, Washington, D. C., 132 pp.

Krishnamurti, T. N., V. Wong, H. L. Pan, G. V. Dam and D. McClellan (1976): Sea surface temperatures for GATE. Florida State University Report 76-3, Dept. of Meteor., Florida State Univ., Tallahassee, Fla., 268 pp.

Kuettner, J. P., D. E. Parker, D. R. Rodenhuis, H. Hoefer, H. Kraus and G. Philander (1974): GATE final international scientific plans. *Bull. Amer. Meteor. Soc.*, 55:711.

Patterson, V. L., M. D. Hudlow, P. J. Pytlowany, F. P. Richards and J. D. Hoff (1978): GATE radar rainfall processing system. NOAA Tech. Memo. CEAS EDIS 26, Washington, D. C., 34 pp.

Rao, M. S. V., W. V. Abbott, III and J. S. Theon (1976): Satellite-Derived Global Oceanic Rainfall Atlas (1973 and 1974). NASA SP-410, Goddard Space Flight Center, National Aeronautics and Space Administration, Greenbelt, Md.

Smith, E. A., and D. R. Phillips (1972): Automated cloud tracking using precisely aligned digital ATS pictures. IEEE Trans. Comput., C-21, New York, N. Y., 715-729.

Smith E. A., and T. H. Vonder Haar (1976): Hourly Synchronous Meteorological Satellite-1 (SMS-1) data collected during the GARP Atlantic Tropical Experiment (GATE). Dept. of Atmos. Sci., Colorado State Univ., Ft. Collins, Colo., 174 pp.

Stout, J. E., D. W. Martin and D. M. Sikdar (1979): Estimating GATE rainfall with geosynchronous satellite images. *Mon. Wea. Rev.*, 107:585.

Wiggert, V., S. S. Ostlund, G. J. Lockett and J. V. Stewart (1976): Computer software for the assessment of growth histories of weather radar echoes. NOAA Tech. Memo. ERL WMPO-35, Boulder, Colo., 86 pp.

Woodley, W. L., A. R. Olsen, A. Herndon and V. Wiggert (1975): Comparison of gage and radar methods of convective rain measurement. *J. Appl. Meteor.*, 14:909.

Appendix

Rainfall Atlas Software

The GATE rainfall atlas software is described here in general terms. Details concerning its use may be obtained by examination of the software, itself.

This software is composed of four program units, SQUISH, SATRACK, TRACER, and RAINMAP, each of which has its own distinct purpose. Among the advantages of this modular approach are: (1) the memory requirements of a computer run are substantially reduced, (2) debugging is simplified, and (3) the meteorological relationships can be changed without all modules having to be rerun.

Although we wanted to make the software as general and flexible as possible, the magnitude of the problem forced us to sacrifice these goals to some extent for the sake of efficiency. The packing of multiple values into a single computer word was used extensively. Packing always diminishes program clarity, but the reduction in core requirements was enormous. The only viable alternative to packing, an overlaying of storage, would have meant much more input/output. Many of the arrays are just big enough to have processed the GATE satellite data to produce the rainfall atlas. Thus, it is possible that for some data cases, arrays would have to be expanded. Probably, such expansion would be necessary in SATRACK.

SQUISH, the first program of the set, prepares an Earth-navigated data array for the other programs. SQUISH, which is heavily oriented towards the Earth-Located Edited Data Set produced for the GATE project, reads the required navigation parameters from this data set to process satellite data from another source, such as the AOIPS tapes produced by NASA. The software can be, and has been, modified to include additional subroutines that derive the navigation variables needed by subroutine SATEAR.

Program SQUISH, as configured, reduces the resolution of the data to 1/3°. SQUISH packs the average temperature and three corresponding threshold counts for the 1/3° bin into a single 60-bit word, if KRUNCH and BINS are changed so that one is working close to full resolution data. It is recommended that the threshold counts be eliminated so that the intrinsic packing can be discarded. Also, at that time, the ISEC array should be converted to type real. These changes greatly enhance program clarity and improve the execution speed. The same changes will also have to be made in SATRACK and RAINMAP.

SATRACK, the second program of the series, has the task of matching clouds between two consecutive pictures. SATRACK's source of input is the Earth-navigated arrays produced by SQUISH. SATRACK's output is the match or status information. The time, area, location, identity, etc., are written for each cloud in each picture. SATRACK has its own restart procedure that allows the tracking phase of processing to be run in segments with all continuity still maintained.

The third program, TRACER, reads as input the data for each cloud in each picture that is produced by program SATRACK. TRACER's function is to link all data for each cloud through its entire lifetime. For TRACER, lifetime is defined as the period from a cloud's appearance in the data until it is lost, perhaps through evaporation or splitting. TRACER then calculates a rain rate for a cloud at each point in its lifetime. Finally, TRACER writes out the rain rate, area, time, and location for each point in the cloud's lifetime. TRACER is the most stable of the four programs and is insensitive to changes in the source or resolution of the satellite data.

RAINMAP, the last of the major programs, requires as input the arrays produced by SQUISH and the linked data produced by TRACER. RAINMAP's function is to reorder the data for each cloud back to a picture-by-picture basis. RAINMAP then apportions the rainfall for each cloud over an output array. RAINMAP presently sums the rainfall for 6 hr before it writes the output array.

To change the method of apportioning rainfall, the most modifications or adjustments must be made in RAINMAP. The ISOLATE subroutine can be changed so as to test various rainfall apportionment schemes. It is possible that some changes would also require a minor corresponding change in TRACER. One such change is to have TRACER write out the rain volumes instead of rain rates.

If the satellite data are from a latitude other than 10° S to 30° N, or if the variable, BINS, is changed to produce a resolution other than 1/3°, additional changes will be necessary. The variables SLAT and WLON in SQUISH control the location of the array ISEC. The AREA function used by SATRACK and RAINMAP must be modified to reflect any change in bin size or location.

The software was written to process either visible or infrared satellite data. The only change that one must make to change data types is to switch the flag IIR. The rest of the changes are taken care of automatically. When visible data are used, however, caution is advised, because the results produced by the visible software have not been thoroughly debugged.

The space requirements of program SQUISH, SATRACK, TRACER, and RAINMAP are 111 K, 145 K, 63 K, and 154 K, respectively. These core sizes are on a CDC 6600 under the KRONOS operating system. Note that the core sizes are specified in octal words. Program SQUISH is by far the largest time consumer. Approximately 85% of the CPU time needed to process the satellite data is used by SQUISH. Conversion of data from satellite coordinates to Earth coordinates is expensive. If execution time is critical, an interpolation scheme could be incorporated into SQUISH. This would decrease the time required for navigation. This becomes increasingly viable if one is working with a high data resolution.

There are also some minor programs for the display of RAINMAP results. These programs are specific, their only function having been to make the products for the GATE atlas. Because they are dependent upon the present software environment of ERL's CDC 6600 in Boulder, they are not included in the software listings.

☆ U.S. GOVERNMENT PRINTING OFFICE: 1979-0-677-096/1209